

A new species of Sebastes (Scorpaeniformes: Sebastidae) from the northeastern Pacific, with a redescription of the blue rockfish, S. mystinus (Jordan and Gilbert, 1881)

The Faculty of Oregon State University has made this article openly available.
Please share how this access benefits you. Your story matters.

Citation	Frale, B. W., Wagman, D. W., Frierson, T. N., Aguilar, A., & Sidlauskas, B. L. (2015). A new species of Sebastes (Scorpaeniformes: Sebastidae) from the northeastern Pacific, with a redescription of the blue rockfish, S. mystinus (Jordan and Gilbert, 1881). (2015). Fishery Bulletin, 113(4), 355-357. doi:10.7755/FB.113.4.1
DOI	10.7755/FB.113.4.1
Publisher	United States Department of Commerce, National Oceanic and Atmospheric Admir
Version	Version of Record
Terms of Use	http://cdss.library.oregonstate.edu/sa-termsfuse



Abstract—The diverse predatory rockfishes (*Sebastes* spp.) support extensive commercial fisheries in the northeastern Pacific. Although 106 species of *Sebastes* are considered valid, many of the ecological, geographical, and morphological boundaries separating them lack clarity. We clarify one such boundary by separating the blue rockfish *Sebastes mystinus* (Jordan and Gilbert, 1881) into 2 species on the basis of molecular and morphological data. We redescribe *S. mystinus*, designate a lectotype, and describe the deacon rockfish, *Sebastes diaconus* n. sp. Aside from its unambiguous distinction at 6 microsatellite loci, the new species is most easily differentiated from *S. mystinus* by its possession of a solid in contrast with a blotched color pattern. *Sebastes diaconus* also possesses a prominent symphyseal knob versus a reduced or absent knob, a flat rather than rounded ventrum, and longer first and second anal-fin spines. *Sebastes diaconus* occurs from central California northward to British Columbia, Canada, and *S. mystinus* occurs from northern Oregon south to Baja California Sur, Mexico, indicating a broad region of sympatry in Oregon and northern California. Further collection and study are necessary to clarify distributional boundaries and to understand the ecology and mechanisms of segregation for this species. Additionally, fisheries assessments will need revision to account for the longstanding conflation of these 2 species.

Manuscript submitted 30 May 2014.
Manuscript accepted 10 June 2015.
Fish. Bull. 113:355–377 (2015)
Online publication date: 9 July 2015.
doi: 10.7755/FB.113.4.1
<http://zoobank.org/References/297E1E76-94C2-49B2-9520-A519B80BC99B>

The views and opinions expressed or implied in this article are those of the author (or authors) and do not necessarily reflect the position of the National Marine Fisheries Service, NOAA.

A new species of *Sebastes* (Scorpaeniformes: Sebastidae) from the northeastern Pacific, with a redescription of the blue rockfish, *S. mystinus* (Jordan and Gilbert, 1881)

Benjamin W. Frable (contact author)^{1, 2}

D. Wolfe Wagman²

Taylor N. Frierson²

Andres Aguilar³

Brian L. Sidlauskas¹

Email address for contact author: ben.frable@oregonstate.edu

¹ Department of Fisheries and Wildlife
Oregon State University
104 Nash Hall
Corvallis, Oregon 97331

² Oregon Department of Fish and Wildlife
Marine Resources Program
2040 SE Marine Science Drive
Newport, Oregon 97365

³ Department of Biological Sciences
California State University, Los Angeles
5151 State University Drive
Los Angeles, California 90032

The rockfish genus *Sebastes* is one of the most diverse and abundant genera along the Pacific coast of North America (Love et al., 2002). Rockfish biology and ecology have been well studied because of their commercial importance, yet some taxonomic limits, population boundaries, and phylogenetic relationships within *Sebastes* remain unclear (Hyde and Vetter, 2007; Orr and Hawkins, 2008) because many species are very similar and overlap in meristic counts and morphometrics. As a result, fishery managers struggle to correctly identify *Sebastes* species and sometimes lack accurate species diagnoses to determine proper management.

Several clusters of similar species within *Sebastes* merit increased taxonomic attention. For example, the uniformly dark-colored species of *Sebastes*, such as the blue rockfish *S.*

mystinus (Jordan and Gilbert, 1881), black rockfish *S. melanops* Girard, 1856, light dusky rockfish *S. variabilis* (Pallas, 1814), and dusky rockfish *S. ciliatus* (Tilesius, 1813), are among the most frequently conflated and confused when landed in the same fishery (Kramer and O'Connell, 1995; Orr and Blackburn, 2004). Even among brightly colored rockfishes, increased study has revealed cryptic species. Gharrett et al. (2005) found 2 genetically distinct forms within the rougheye rockfish *S. aleutianus* (Jordan and Evermann, 1898), and those forms were later designated as the rougheye rockfish *S. aleutianus* and blackspotted rockfish *S. melanostictus* (Matsubara, 1934) (Orr and Hawkins, 2008). The historical concept of the vermilion rockfish *S. miniatus* (Jordan and Gilbert, 1880a) was also shown relatively recently to

include 2 reproductively isolated entities (Hyde, et al., 2008).

In this study, we focus taxonomic attention on *S. mystinus*, a common nearshore species found from northern Mexico to British Columbia, Canada. In the 19th century, *S. mystinus* was the most commercially important species in California; now it is mainly targeted recreationally (Love et al., 2002). Over the last decade, multiple studies have identified 2 genetically distinct groups of *S. mystinus* along the Pacific coast (Cope, 2004; Burford and Larson, 2007; Burford and Bernardi, 2008; Burford, 2009; Burford et al., 2011a, 2011b), and in several studies the presence of 2 morphologically unrecognized species have been hypothesized (Burford and Bernardi, 2008; Burford, 2009; Burford et al., 2011a, 2011b).

Cope (2004) first identified genetic distinctions between northern and southern populations of blue rockfish while studying their stock structure. His analysis revealed numerous fixed differences in the sequence of the mitochondrial control region between samples from the Oregon–Washington region and samples from California waters. These data indicate that the genetic break occurred in the vicinity of Cape Mendocino, California.

Burford and colleagues then applied additional molecular and phylogeographic analyses to these 2 populations (Burford and Larson, 2007; Burford and Bernardi, 2008; Burford, 2009; Burford et al., 2011a, 2011b). In a combined analysis of mitochondrial (control region) and nuclear (recombination-activating gene 1 [RAG1]) markers and microsatellites for the subgenus *Sebastes*, Burford and Bernardi (2008) were the first to propose that the 2 populations might represent different species. Within *S. mystinus*, Burford and Bernardi (2008) identified 2 clades with higher genetic divergence ($F_{ST}=0.120$) than that found between 2 well-established species (Narum et al., 2004), the gopher rockfish *Sebastes carnatus* (Jordan and Gilbert, 1880b) and the black-and-yellow rockfish *S. chrysomelas* (Jordan and Gilbert, 1881), and with much higher genetic divergence than that among populations of *S. melanops* ($F_{ST}=0.032$) (Miller et al., 2005). They estimated the divergence time of the 2 lineages to be between 780,000 and 920,000 years ago, far preceding the Last Glacial Maximum (LGM) and, therefore, refuting Burford and Larson's (2007) hypothesis that the LGM caused allopatric speciation within *S. mystinus*.

Burford and Bernardi (2008) concluded that the 2 genetically distinct groups of *S. mystinus* are incipient species on the basis of the evidence presented here previously and the lack of evidence for introgression or hybridization. Burford (2009) expanded on this conclusion by directly testing hypotheses of demographic history and speciation scenarios with an expanded sampling of 6 microsatellites and the control region marker. They found evidence for a demographic contraction and rapid expansion near the time of genetic coalescence and far earlier than the LGM (Burford, 2009). Burford (2009) concluded that the 2 lineages speciated allopatrically

much earlier than the LGM and that they have subsequently expanded ranges to form an area of sympatry from central Oregon to northern California.

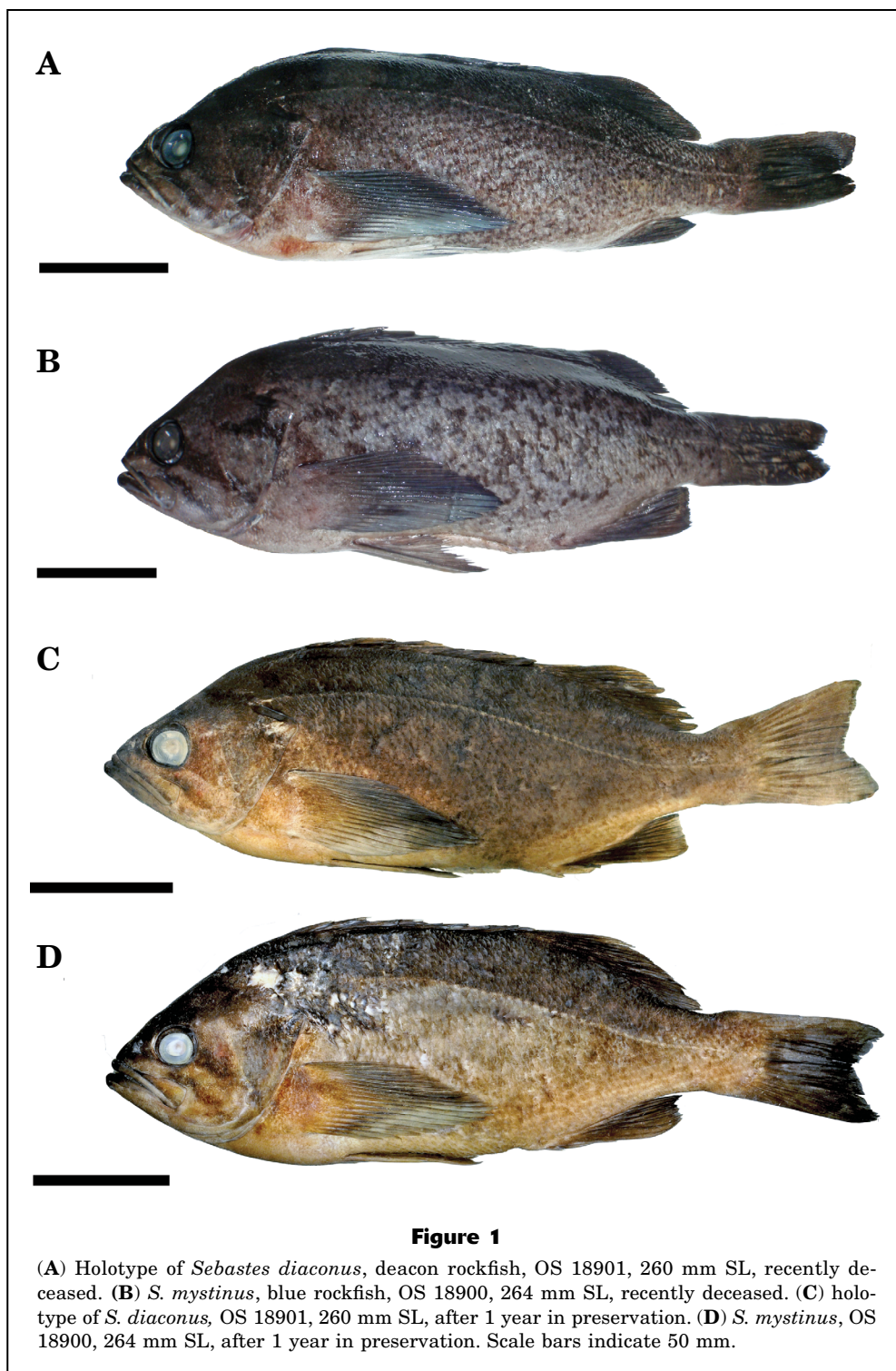
Finally, Burford et al. (2011a, 2011b) examined microsatellite data from 466 type-1 (northern group) and 1752 type-2 (southern group) specimens collected from Fort Bragg, California, south to Santa Cruz Island, California, to determine rates of hybridization (Burford et al., 2011a) and year-class compositional and ecological differences (Burford et al., 2011b). Burford et al. (2011a) found no hybridization in northern localities with higher co-occurrence, but they identified low levels in Southern California (highest rate of hybridization=4.1%). This finding, combined with the identification of a Wahlund Effect (i.e., lower heterozygosity than expected at random between the 2 populations), indicates that reproductive isolation helps maintain the segregation, especially in areas of overlap (Burford et al., 2011a). Burford et al. (2011a, 2011b) considered their results to provide sufficient evidence that the 2 genetic lineages are cryptic rather than incipient species.

Despite the accumulating detail on genetic differentiation, no study provided a complementary physical description of the 2 types. Because of the lack of physical descriptions or defining characteristics, precise field identification of Burford's genetic lineages (type 1 and type 2) has eluded biologists and fishermen alike.

Meanwhile, fisheries biologists acknowledged 2 different trunk pigmentation patterns in *S. mystinus* from near the Oregon, Washington, and California shores: the "blue-sided" (Fig. 1, A and C) and "blue-blotched" rockfishes (Fig. 1, B and D) (Love, 2011), which, as the authors of the earlier genetic studies have indicated, match the type-1 and type-2 genetic lineages, respectively (Burford¹). That difference in color pattern indicates that these lineages may be more morphologically distinguishable than originally thought.

The wealth of recent genetic work on *S. mystinus* and the discovery of a color polymorphism that is congruent with the major genetic break indicate that a formal taxonomic reevaluation is overdue. In this study, we 1) test whether the morphotypes correspond with the types of Burford and Bernardi (2008), 2) characterize the morphological features of the 2 genetic types, 3) use genetic and morphological data to evaluate species status, and 4) clarify the geographic ranges of the 2 forms. In doing so, we confirm the genetic separation of the 2 color morphs and provide a formal description of the type-1 or blue-sided form as a new species, *S. diaconus*, the deacon rockfish. The type-2 or blue-blotched form matches most of the original syntype series of *S. mystinus*, from which we designate a lectotype and re-describe the species. This study provides information essential to proper population monitoring and management of these species in Oregon and the northeastern Pacific.

¹ Burford, M. 2012. Personal commun. Department of Applied Ecology, North Carolina State Univ., Raleigh, NC 27695.



Materials and methods

Samples

Type material and preserved specimens were examined from 6 ichthyology collections containing major

holdings from the northeastern Pacific: CAS, UBC, LACM, UWFC, OS, and USNM (collection abbreviations sensu Sabaj Pérez, 2013). Fresh specimens were collected by DWW and TNF with hook and line from nearshore reefs (13–29 m deep) off the central Oregon coast (44°44′12.30″N, 124°4′33.59″W to 44°24′11.74″N,

124°13'55.56"W) from 9 April to 25 June 2012 under the annual scientific collecting permit issued by the Oregon Department of Fish and Wildlife (ODFW) for the collection of samples by their employees (DWW and TNF). Specimens were frozen for transport, thawed, and photographed. Samples of tissue from the trunk musculature were removed and archived, and 35 of these freshly collected samples (*S. mystinus* [$n=15$], *S. diaconus* [$n=20$]) were genotyped during microsatellite analysis. Voucher specimens were fixed in 10% formalin, preserved in 50% isopropanol, cataloged, and deposited in the Oregon State Ichthyology Collection (OS). More detailed information on catalog number, collection locality, and size of each examined specimen appears in the species descriptions that follow. We examined 134 specimens for comparisons of meristic and linear morphometric data: *S. mystinus* ($n=68$), *S. diaconus* ($n=58$), *S. ciliatus* ($n=6$), and *S. variabilis* ($n=2$).

Genetic sampling

Muscle tissue was used to extract DNA from 15 blue-blotched and 20 blue-sided individuals with DNeasy² blood and tissue kits (Qiagen, Valencia, CA). Microsatellite loci were amplified by a 3-primer polymerase chain reaction (PCR) protocol (Schuelke, 2000). To test the assignment of the color morphotypes with the previously described genetic groups, 16 type-1 and type-2 individuals previously identified and analyzed by Burford and Bernardi (2008) were included in microsatellite amplification and analysis.

Amplification of microsatellite markers and DNA sequences

We amplified 6 anonymous microsatellite markers (*Seb37*, Roques et al., 1999; *Spi4*, Gomez-Uchida et al., 2003; *Sra7-7*, *Sra15-8*, Westerman et al., 2005; *Ssc69*, Yoshida et al., 2005; and *KSs18A*, An et al., 2009). Two microsatellite loci (*Sra7-7* and *Sra15-8*) were used by Burford and Bernardi (2008) in the original description of the 2 lineages. The 3-primer amplification protocol was used to run in 15- μ L volumes with the following reaction concentrations: 1 \times AmpliTaq PCR Buffer (Thermo Fisher Scientific, Inc., Waltham, MA) buffer, 2.5 mM MgCl₂, 0.4 mM of each dNTP, 2.7 $\times 10^{-4}$ mg/mL BSA, 0.3 μ M reverse primer, 0.3 μ M fluorescently labeled M13 sequence (5'CACGACGTTGTAACGAC3') with dye labels (FAM, VIC, NED, PET; Thermo Fisher Scientific, Inc.), 0.07 μ M M13 5'-end labeled forward primer, 0.2 units of AmpliTaq DNA polymerase, and 5 μ L DNA (5–20 ng/ μ L). We used the following thermal profile: initial denaturing step at 94°C for 5 min, followed by 30 cycles of 94°C for 30 s, 52°C for 30 s, and 72°C for 45 s. The incorporation of the M13 prim-

er required 15 cycles of 94°C for 30 s, 48°C for 30 s, and 72°C for 45 s. A 7-min extension after the final cycle completed the thermal profile. Amplified products were run on an Applied Biosystems 3100 automated sequencer with GeneScan 500 LIZ Size Standard and genotyped with GeneMapper, vers. 3.7 (Thermo Fisher Scientific, Inc.).

Analysis of microsatellite markers and DNA sequence

We used the software program Structure, vers. 2.3 (Falush et al., 2003; Pritchard et al., 2000) to determine the correspondence of blue-sided and blue-blotched morphotypes with the type-1 and type-2 genetic groups described by Burford and Bernardi (2008). Parameters in Structure were set to produce posterior probabilities with 500,000 replicates recorded after a burn-in period of 50,000 steps that were discarded. Default settings were used with the admixture option in Structure. Because the optimal K value was previously identified as 2 (Burford and Bernardi, 2008), we ran simulations according to these parameters to identify the corresponding genetic groups of each morphotype. We also simulated structure runs with K values within a range of 2–4 and identified optimal K value with the online program Structure Harvester, vers. 6.92 (Earl and vonHoldt, 2012).

Measurements and meristics

Measurements were taken to the nearest 0.01 mm with digital calipers. Morphometrics (32 measurements) and meristics (17 counts) followed Orr and Hawkins (2008), except as follows. Symphyseal knob length was measured on the ventral side of the lower jaw from the posterior margin of the symphysis to the anterior tip of the knob. Head depth was measured along the vertical bisecting the eye. An additional point-to-point measurement was taken from the dorsal-fin origin to anal-fin origin. We augmented the meristics used by previous authors with counts of dorsal-fin spines, of branched and unbranched pectoral-fin rays on both sides of the fish, of transverse lateral scale rows, and of posterior and anterior gill rakers from the left side of the fish. Dorsal-, anal-, pectoral- and pelvic-fin rays and spines were counted from preserved specimens. Vertebrae and caudal-fin rays were counted from a subsample of specimens ($n=68$) via film radiographs.

Morphometric analysis

We created a size-standardized morphospace for 120 specimens (6 specimens were excluded because of damage) with the Allometric Burnaby technique (Burnaby, 1966) implemented in the software PAST, vers. 2.17 (Hammer et al., 2001), which log transforms the 32 linear measurements and projects them orthogonally to the first principal component. These data were then used in a principal components analysis (PCA). For statistical analyses, putative species membership

² Mention of trade names or commercial companies is for identification purposes only and does not imply endorsement by the National Marine Fisheries Service, NOAA.

was assigned a priori on the basis of trunk color pattern (blotched versus solid). To allow for the inclusion of juveniles, which lack distinguishing color patterns, and for faded long-preserved specimens in the morphometric analysis, we assigned specimens from extreme ends of the known geographic ranges to the only species known to occur in such regions. No ambiguous juveniles or faded specimens from the known region of geographic overlap were included in morphometric analysis.

The overall morphometric distinctiveness of the 2 putative species was tested by inputting the eigenvectors that explained the greatest percent variance from the PCA into a multivariate analysis of variance (MANOVA) implemented in PAST software. The significances of differences between the means of putative species ($P \leq 0.05$) on each axis were tested with pairwise post-hoc comparisons, by using Tukey's honestly significant difference (HSD) test. A discriminant function analysis (DFA, also implemented in PAST) was used to further determine which morphometric measurements best separated the species. The robustness of the DFA to assign the data to a priori groupings was evaluated with a leave-one-out cross-validation in PAST. Results of this procedure are reported in percentages assigned to the same a priori grouping. The untransformed versions of the 32 variables that explained the highest proportion of variance in the DFA were regressed against length (standard length [SL]) for each species to determine whether the traits differed allometrically or isometrically. This comparison of allometric trajectories was performed in the *smatr* package (Warton et al., 2012) in R, vers. 3.0.1 (R Core Team, 2013). Linear regressions were plotted with the *ggplot2* package in R (Wickham, 2009). Some individual linear morphometric measurements were compared to determine statistical significance with a 2-tailed Student's *t*-test for unequal frequencies implemented in R.

Results

Genetic analysis

When K was 2, all of the individuals genotyped from this study were assigned high ancestry (>90%) with 1 of the 2 clusters (Fig. 2). The specimens identified as *S. diaconus* or blue-sided sensu Love (2011) clustered unambiguously with the type-1 blue rockfish and the *S. mystinus* or blue-blotched individuals clustered with the type-2 blue rockfish of Burford and Bernardi (2008) (Fig. 2), thereby confirming that the color polymorphism reliably separates the genetic types.

Morphometric analysis

Principal component analysis of size-standardized linear morphometric variables for specimens with clear a priori classification (see the *Materials and methods* section) revealed overlap between the 2 putative spe-

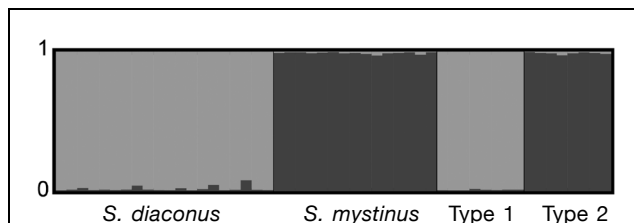


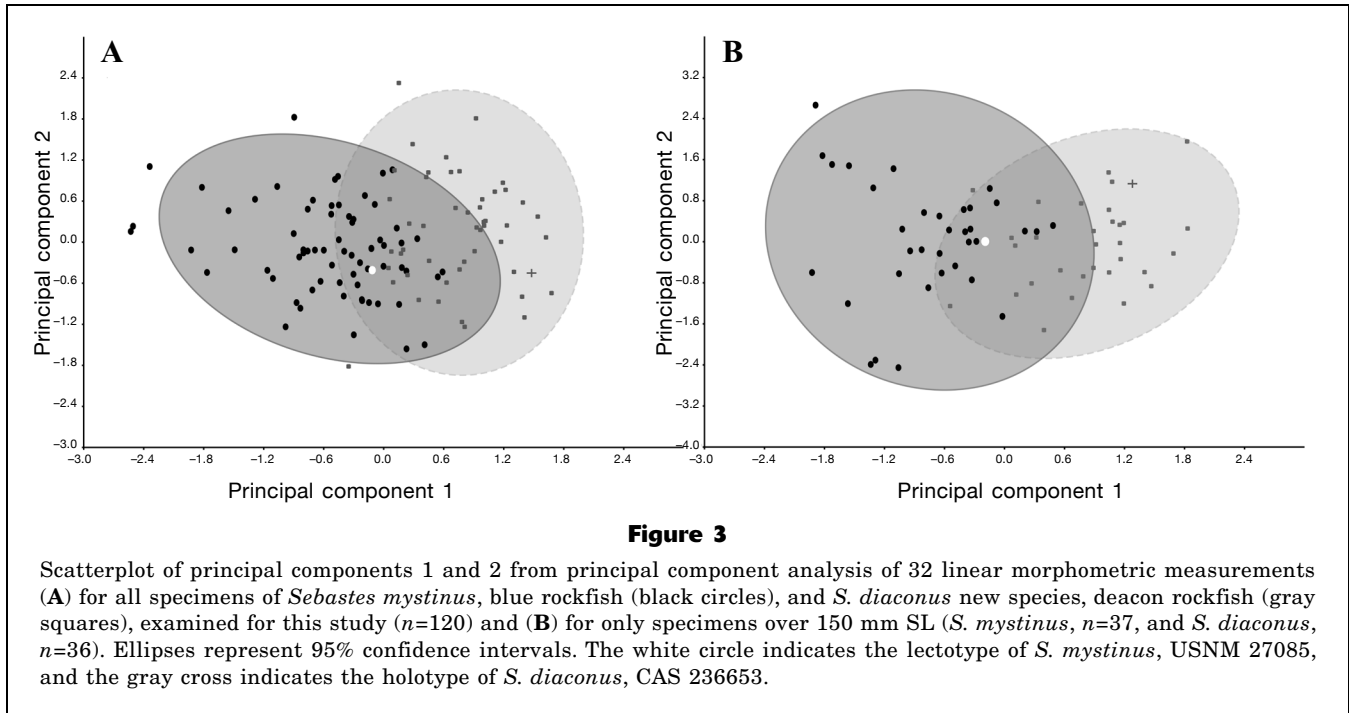
Figure 2

Structure plot derived from microsatellite data showing genetic group assignments of specimens of *Sebastes diaconus* (deacon rockfish; $n=20$) and *S. mystinus* (blue rockfish; $n=15$) from this study (on left) compared with specimens previously genotyped by Burford and Bernardi (2008) (on right), type 1 ($n=8$) and type 2 ($n=8$) with a K value of 2. Each bar represents one individual with color corresponding to population assignment.

cies (Fig. 3) but a clear difference in mean phenotype ($P < 0.0001$, MANOVA on first 4 axes explaining 51.0% of total variance). Percent variance explained dropped after PC4 (Fig. 4A). The most discrimination was offered by PC1 (17.1% of variance; Table 1), with blue-sided individuals, or *S. diaconus*, having on average more positive scores than members of *S. mystinus*, or the blue-blotched phenotype (Fig. 3). The variables with the highest loadings along PC1 were symphyseal knob length, the lengths of the first 2 anal-fin spines, and the length of the first dorsal-fin spine (Table 1). Explaining 12.1% of variance, PC2 primarily indexes variation in suborbital depth, anal-fin spine I length, and the dorsal and ventral lengths of the caudal peduncle (Table 1). Pairwise Tukey's HSD tests recovered significant differences between the 2 species on PC1 ($P = 0.0001$) but not on the subsequent axes.

When individuals under 150 mm SL were removed from the data set, the percent variance explained by the first 2 principal components (PCs) increased (Fig. 4B). For PC1 (23.1% of total variance), the main measurements of variation were symphyseal knob length, anal-fin spines I and II lengths, and ventral caudal peduncle length (Table 1), and, for PC2 (13.4% of total variance), the largest loadings were for symphyseal knob length and lengths of anal-fin spines I, II and III (Table 1). As with the analysis of the complete data set, the multivariate means of the 2 species differed significantly (MANOVA, $P < 0.001$): only the analysis of PC1 revealed a significant morphometric difference in the pairwise Tukey's HSD tests ($P = 0.001$).

The depth at dorsal-fin origin, pelvic-fin ray length, preanal fin length, and dorsal-fin origin to anal-fin origin received the highest weight in the linear discriminant equation of the variation between the 2 species (Table 2) in the size-standardized morphospace. This discriminant function correctly reclassified all but 2 individuals in a leave-one-out cross-validation (98.3% correct reclassification; Fig. 5A). The exclusion of juveniles under 150 mm SL improved the performance of



the DFA and yielded a linear equation permitting 100% correct reclassification of 73 adult specimens (Fig 5B). The coefficients for head length (HL) and prepelvic fin length increased substantially in the discriminant function that was restricted to individuals over 150 mm SL, in comparison with the function including specimens of all sizes (Table 2).

Between-group comparison of type-II regressions of the untransformed measurements with the highest loadings on size-standardized PC1 against SL indicated significantly different slopes for the lengths of anal-fin spine I ($P<0.001$) and anal-fin spine II ($P=0.002$), for symphyseal knob length ($P<0.001$), and for ventral caudal peduncle length ($P=0.003$). Linear regressions of these 4 variables against SL illustrate the differences in slope (Fig. 6, A–D). It appears that the 2 species are morphometrically similar at smaller sizes yet differentiate interspecifically as they age, with the symphyseal knob length (Fig. 6A) and the lengths of the anal-fin spines (Fig. 6, B and C) diverging substantially in specimens over 150 mm SL. Ventral caudal peduncle length diverges less pronouncedly (Fig 6D).

On the basis of the morphometric differences discovered in this study, the differences in body coloration, and the correspondence of the morphotypes with previously identified genetic groups, we recognize the 2 genetic lineages within the previous concept of *S. mystinus* as full species. We describe *S. diaconus*, or the type-1 or blue-sided form, as new; we restrict *S. mystinus* to the type-2 or blue-blotched form; and we redescribe the latter species and designate a lectotype and paralectotypes.

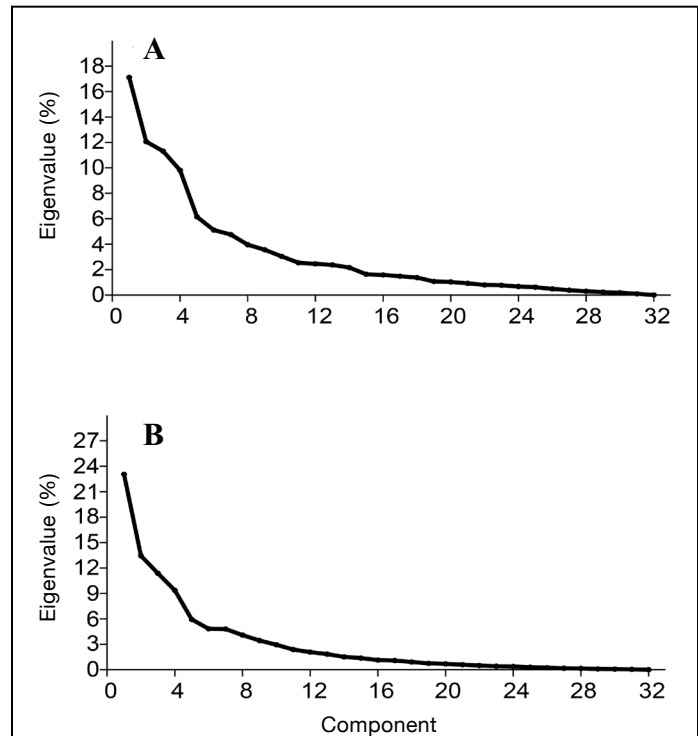


Table 1

Variable loadings and percent variance explained for the first 4 principal component axes of a principal component analysis for morphometric measurements of all specimens examined for this study, *Sebastes mystinus* (blue rockfish; $n=68$) and *S. diaconus* (deacon rockfish; $n=52$) combined, and of specimens over 150 mm SL, *S. mystinus* ($n=37$) and *S. diaconus* ($n=36$) combined. Highest loadings are indicated in bold.

Measurement	All specimens				Specimens over 150 mm SL			
	Axis 1	Axis 2	Axis 3	Axis 4	Axis 1	Axis 2	Axis 3	Axis 4
Percent variance explained	17.113	12.066	11.313	9.813	23.055	13.443	11.373	9.362
Head length	0.061	0.017	-0.031	0.126	0.110	-0.003	-0.007	0.165
Orbit length	0.094	0.046	-0.003	0.106	0.115	0.003	-0.081	0.153
Snout length	0.036	-0.027	0.123	-0.370	-0.041	0.040	0.249	-0.347
Interorbital width	-0.081	-0.023	-0.072	-0.010	-0.107	0.001	-0.040	0.029
Suborbital depth	-0.194	-0.586	0.564	-0.285	-0.181	0.061	-0.531	-0.700
Head depth	-0.086	-0.049	-0.207	0.162	-0.140	-0.133	-0.214	0.174
Upper jaw length	0.010	-0.024	-0.019	-0.018	-0.026	-0.008	0.084	0.027
Lower jaw length	0.098	0.018	0.019	0.083	0.132	-0.021	-0.002	0.011
First gill arch length	-0.017	0.033	-0.072	0.359	0.051	0.031	-0.313	0.392
Symphyseal knob length	0.818	-0.273	-0.267	-0.242	0.637	-0.625	0.099	-0.193
Predorsal fin length	0.040	0.000	0.026	-0.031	0.035	-0.017	0.036	0.001
Prepelvic fin length	0.009	-0.097	0.000	0.119	0.023	-0.067	-0.136	0.057
Preanal fin length	-0.035	-0.056	-0.034	0.105	-0.019	-0.045	-0.068	0.112
Depth at dorsal fin origin	-0.114	-0.051	-0.065	0.129	-0.101	-0.021	-0.074	0.091
Depth at pelvic fin origin	-0.094	-0.049	-0.084	0.179	-0.078	-0.039	-0.118	0.137
Depth at anal fin origin	-0.049	-0.053	-0.114	0.096	-0.051	-0.060	-0.017	0.043
Dorsal-fin spine I length	0.073	0.160	0.038	-0.144	0.009	0.130	0.115	0.074
Dorsal-fin spine IV length	0.083	0.066	-0.006	0.048	0.099	0.074	0.082	0.072
Spinous dorsal-fin base length	-0.044	-0.136	-0.072	0.175	-0.036	-0.059	-0.144	0.147
Soft rayed dorsal-fin base length	-0.084	0.011	-0.056	-0.044	-0.078	-0.109	-0.033	-0.017
Pectoral-fin base depth	-0.125	-0.067	-0.052	0.001	-0.138	-0.020	0.084	-0.028
Pectoral fin length	-0.100	-0.088	-0.020	-0.020	-0.116	-0.040	0.049	0.012
Pelvic-fin ray length	-0.109	0.030	-0.015	-0.109	-0.144	0.007	0.115	-0.027
Pelvic-fin spine length	-0.058	0.136	0.145	-0.032	-0.040	0.149	0.144	0.074
Anal-fin base length	0.005	0.030	-0.015	0.034	0.028	0.045	0.060	-0.010
Anal-fin spine I length	0.273	0.450	0.574	0.152	0.477	0.628	-0.016	-0.044
Anal-fin spine II length	0.147	0.146	0.193	0.203	0.251	0.237	-0.049	-0.066
Anal-fin spine III length	0.085	0.109	0.222	0.033	0.083	0.202	0.125	-0.062
Dorsal fin origin to anal fin origin	-0.066	-0.051	-0.044	0.108	-0.058	0.002	-0.060	0.122
Caudal peduncle depth	-0.093	0.003	-0.063	0.007	-0.125	-0.009	0.035	-0.021
Caudal peduncle dorsal length	-0.173	0.444	-0.222	-0.479	-0.180	-0.066	0.531	-0.072
Caudal peduncle ventral length	-0.132	0.189	-0.096	-0.270	-0.200	0.115	0.221	-0.016

Sebastes diaconus, new species

Proposed English common name: deacon rockfish

Figures 1, A and C, 2–6, 7A, 8A, 9, and 10; Tables 1–3.

Kramer and O’Connell, 1995:45 (in part); Mecklenburg et al., 2002:360; Love et al., 2002:215 (in part); Love, 2011:250–251 (in part).

Sebastichthys mystinus Jordan and Gilbert, 1881: Bean, 1882:26 (presence in Puget Sound, Washington]; Goode, 1884:266 (in part, mention of fishes from Vancouver Island, Canada, and Puget Sound; having affinity with *Sebastes melanops* in Puget Sound).

Sebastodes mystinus (Jordan and Gilbert, 1881): Whiteaves, 1887:135 (first record of capture in Canada); Jordan and Evermann, 1898:1785 (in part, presence in Puget Sound); Phillips, 1957:52–53 (in part); Clemons and Wilby, 1961:252–253.

Sebastes mystinus (Jordan and Gilbert, 1881): Hart, 1973:429; Eschmeyer and Herald, 1983:144 (in part);

Holotype

OS 18901, 260 mm SL, 1.8 km west of Seal Rock, OR, 44°29’49.38”N, 124°6’30.48”W, 20.9 m depth, 20 April 2012, D. W. Wagman and T. N. Frierson.

Paratypes

CAS 25336, 1, 153 mm SL, off Point Diablo, San Francisco, CA, 2 August 1947, W. I. Follett, C. O. Garrels, and C. F. Maertins; LACM 31942.008, 6, 240–266 mm SL, northeast of Redding Rock, Humboldt County, CA,

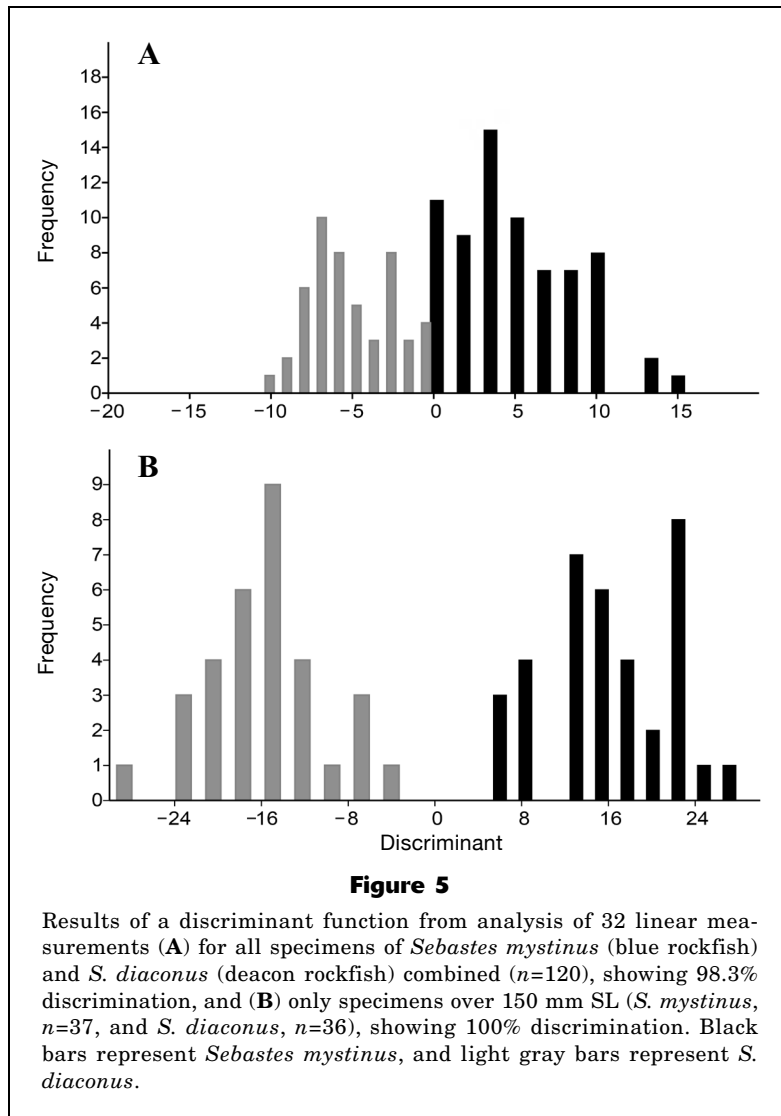
Table 2

Discriminant functions for morphometric measurements determined by a discriminant function analysis for all individuals, *Sebastes mystinus* (blue rockfish; $n=68$) and *S. diaconus* (deacon rockfish; $n=52$) combined, and for individuals over 150 mm SL, *S. mystinus* ($n=37$) and *S. diaconus* ($n=36$). Most extreme coefficients are indicated in bold.

Measurement	All individuals	Individuals over 150 mm SL
Head length	36.018	-448.42
Orbit length	27.157	-219.98
Snout length	44.661	-214.68
Interorbital width	30.4	-289.5
Suborbital depth	43.81	-275.26
Head depth	37.254	-235.15
Upper jaw length	30.458	-275.91
Lower jaw length	31.126	-206.71
First gill arch length	36.431	-138.46
Symphyseal knob	0.88836	-321.07
Predorsal fin length	33.422	-261.83
Prepelvic fin length	34.419	-487.52
Preanal fin length	88.378	28.582
Depth at dorsal fin origin	89.738	-125.6
Depth at pelvic fin origin	34.136	-276.5
Depth at anal fin origin	13.885	-241.26
Dorsal-fin spine I length	57.141	-129.78
Dorsal-fin spine IV length	31.63	-213.65
Spinous dorsal-fin base length	60.405	9.4878
Soft rayed dorsal-fin base length	44.333	-171.56
Pectoral-fin base depth	55.919	-367.57
Pectoral fin length	48.979	-248.9
Pelvic-fin ray length	85.235	-150.96
Pelvic-fin spine length	49.767	-64.665
Anal-fin base length	27.607	-242.01
Anal-fin spine I length	15.63	-175.03
Anal-fin spine II length	-8.2368	-367.43
Anal-fin spine III length	12.647	-235.56
Dorsal fin origin to anal fin origin	110.32	-270.45
Caudal peduncle depth	42.199	-218.95
Caudal peduncle dorsal length	23.46	-243.75
Caudal peduncle ventral length	45.236	-152.4

15.4 m depth, 4 August 1971, McBean et al.; OS 18882, 1, 160 mm SL, 1.4 km west of Tokatee Kloochman State Natural Site, OR, 44°12'26.28"N, 124°8'2.04"W, 19.2 m depth, 24 April 2012, D. W. Wagman and T. N. Frierson; OS 18883, 1, 218 mm SL, 1.8 km southeast of Seal Rock, OR, 44°29'4.20"N, 124°6'14.62"W, 17.9 m depth, 7 May 2012, D. W. Wagman and T. N. Frierson; OS 18884, 4, 190–272 mm SL, 2.9 km west of Ona Beach State Park, OR, 44°31'8.94"N, 124°7'2.96"W, 15.2 m depth, 7 May 2012, D. W. Wagman and T. N. Frierson; OS 18885, 2, 125 and 235 mm SL, 1.8 km west Ona Beach State Park, OR, 44°31'27.98"N, 124°6'6.55"W, 16.5 m depth, 8 May 2012, D. W. Wagman and T. N. Frierson; OS 18888, 1, 125 mm SL, 2.1 km west of Lost Creek State Park, OR, 44°33'14.83"N, 124°6'1.94"W, 8 May 2012, 13.2 m depth, D. W. Wagman and T. N. Frierson; OS 18889, 3, 140–188 mm SL, 2.0 km west of Lost Creek State Park, OR, 44°33'16.34"N, 124°6'0.04"W, 13.2 m depth,

15 May 2012, D. W. Wagman and T. N. Frierson; OS 18890, 3, 164–292 mm SL, 1.1 km west of Lost Creek State Park, OR, 44°33'21.96"N, 124°5'20.36"W, 14.5 m depth, 20 April 2012, D. W. Wagman and T. N. Frierson; OS 18893, 1, 225 mm SL, 1.8 km west of north end of Lost Creek State Park, OR, 44°33'37.51"N, 124°5'45.82"W, 18.8 m depth, 8 May 2012, D. W. Wagman and T. N. Frierson; OS 18895, 2, 230 and 270 mm SL, 1.8 km northwest of Lost Creek State Park, OR, 44°33'57.17"N, 124°5'43.26"W, 14.3 m depth, 8 May 2012, D. W. Wagman and T. N. Frierson; OS 18897, 1, 259 mm SL, 3.2 km southwest of South Beach State Park, OR, 44°34'49.98"N, 124°6'18.94"W, 19.0 m depth, 7 May 2012, D. W. Wagman and T. N. Frierson; UW 44179, 1, 330 mm SL, off Ozette Island, WA, 9.1 m depth, collector and date unknown; UW 44330, 1, 246 mm SL, off Neah Bay, WA, 29 January 1993, Seattle Aquarium.



Additional nontype material

CAS 18799, 1, 128 mm SL, Off Santa Cruz Island, CA, 29 August 1954, E. Hunter; CAS 25976, 1, 104 mm SL, Southeast Farallon Island, CA, 8 May 1949, G. D. Hanna and A. G. Smith; CAS 27910, 2, 67–93 mm SL, Arena Cove, Mendocino, CA, 38°54'51"N, 123°42'55"W, 8.5–9.1 m depth, 8 April 1973, R. N. Lea et al.; CAS 28487, 1, 65 mm SL, Arena Cove, Mendocino, CA, 8 April 1973, R. N. Lea et al.; SU 11776, 1, 228 mm SL, Monterey, CA, December 1895, D. S. Jordan; SU 15112, 3, 63–117 mm SL, Pacific Grove, pier at far end of city beach, CA, 3 August 1948, C. Limbaugh, A. Flechzig, and E. Walker; LACM 31938.002, 6 of 27, 52–120 mm SL, St. Georges Reef, Whale Rock, Del Norte, CA, 10.7–13.7 m depth, 2 August 1971, D. Gotshall, D. Odenweiler, C. Swift, and D. Clifton; OS 1252, 2, 130–140 mm SL, beyond Yaquina Bay Bridge, OR, 27 May 1962, H. Murray; OS 4162, 1, 250 mm SL, Pacific Ocean off mouth of Columbia River,

OR, 9 May 1961, P. Wolf; OS 7466, 107 mm SL, Pacific Ocean off Tillamook County, OR, 45°15.7'N, 124°0.6'W, 36.6 m depth, RV *Cayuse*, cruise C-7805-D, station 8, haul SBMT 224, 16 May 1978, E. E. Krygier; OS 11176, 1, 48 mm SL, off Oregon, 43°37'N, 124°15'W, 36.6 m depth, 28 June 1978, collector unknown; UW 1559, 1, 168 mm SL, Farallon Islands, CA, 26 October 1922, C. L. Hubbs; UW 40703, 3 of 6, 71–111 mm SL, Monterey Bay, CA, 7 October 1953, W. I. Follett.

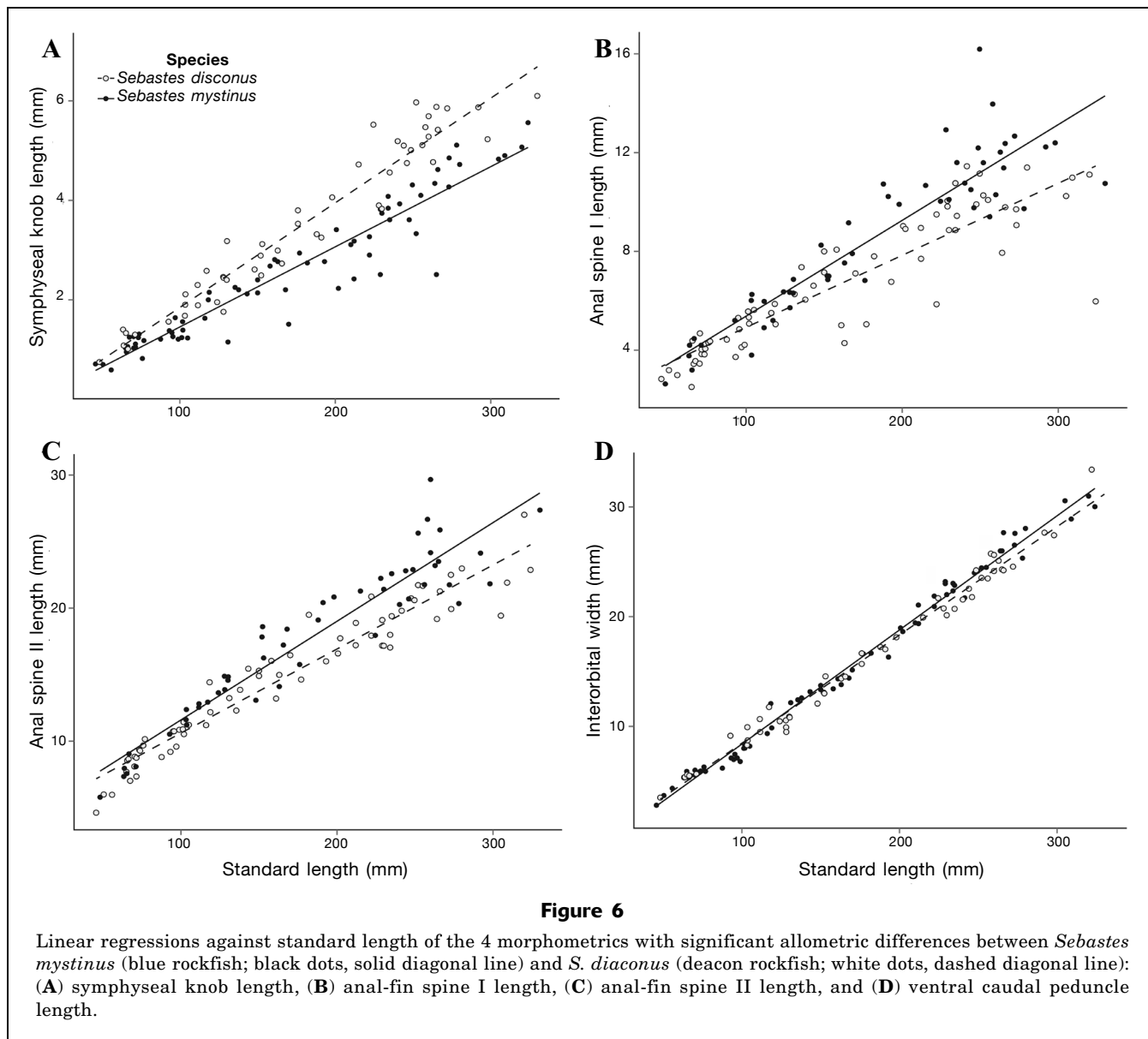
Diagnosis

A species of *Sebastes* differentiated from all congeners, except *S. ciliatus*, *S. melanops*, and *S. mystinus*, by possession of dark gray, blue, brown, or black body coloration, scales that cover the mandible, and weak or absent head spination. *Sebastes diaconus* can be distinguished from *S. ciliatus* and *S. melanops* by the maxilla not extending beyond the posterior margin of the pupil when the mouth is closed. It is further distinguished from *S. ciliatus* by 4 bars of dark pigmentation that extend across the head and nape, versus the almost uniformly dark head coloration with 2 faint bars below the orbit in *S. ciliatus*, and by 26–27 vertebrae versus 28–29 vertebrae in *S. ciliatus*. *Sebastes diaconus* is further distinguished from *S. melanops* by having a uniform, light blue-gray, speckled pattern on the trunk, versus the darker black-gray coloration with irregular areas of dark pigmentation ranging from speckling to blotches in *S. melanops*, and by having dark dorsal-fin membranes without dark spots. *Sebastes diaconus* is most easily distinguished from *S. mystinus* by a brownish-blue to blue-gray trunk with distinct lighter blue-gray speckles versus the steel-blue to greenish-blue body coloration and large, dark blotches (also apparent in preserved specimens) of *S. mystinus*; this character is indistinct in many individuals under 100 mm SL. In specimens over 150 mm SL, *S. diaconus* can be further distinguished from *S. mystinus* by having the ventral margin of head and ventrum generally flat versus rounded and by the allometric development of the symphyseal knob (length of dentary symphysis 4.0–7.0% HL vs. 2.6–5.7% HL in *S. mystinus*). Although these ratios overlap, the symphyseal knob length differs diagnostically among specimens of equal size over 150 mm SL. This measurement can be diagnosed by comparison with allometric plots (Fig. 6A).

distinct lighter blue-gray speckles versus the steel-blue to greenish-blue body coloration and large, dark blotches (also apparent in preserved specimens) of *S. mystinus*; this character is indistinct in many individuals under 100 mm SL. In specimens over 150 mm SL, *S. diaconus* can be further distinguished from *S. mystinus* by having the ventral margin of head and ventrum generally flat versus rounded and by the allometric development of the symphyseal knob (length of dentary symphysis 4.0–7.0% HL vs. 2.6–5.7% HL in *S. mystinus*). Although these ratios overlap, the symphyseal knob length differs diagnostically among specimens of equal size over 150 mm SL. This measurement can be diagnosed by comparison with allometric plots (Fig. 6A).

Description

Description based on 58 specimens, 48.2–344.0 mm SL. Counts and measurements of holotype and ranges, av-



erages, and standard deviations for all specimens are provided in Table 3. Values in parentheses represent modes for meristic counts and means for morphometric ratios.

Dorsal-fin spines XXII or XXIII (XXIII), rays 14–17 (16); anal-fin spines III, rays 8 or 9 (9); pectoral-fin unbranched rays 9–10 (10), branched rays 6–8 (8), total pectoral rays 16–18 (18); pelvic-fin spines 1; pelvic-fin rays 5; total caudal-fin rays 38–41 (39); dorsal segmented caudal rays 8; ventral segmented caudal rays 8; dorsal procurrent caudal rays 11–13 (12); ventral procurrent caudal rays 11–12 (11); total vertebrae 26, rarely 27; anterior gill rakers 28–35 (33); posterior gill rakers 21–26 (22); scales ctenoid; lateral line complete and pronounced, lateral-line pores 41–51 (45); scales in lateral series on midline 56–68 (62).

Body deep and ellipsoid; depth at pelvic-fin origin 25.4–39.5% SL (34.4% SL); depth at anal-fin origin 22.0–34.8% SL (29.6% SL), lowest values in smallest specimens; depth at dorsal-fin origin 24.7–36.8% SL (33.5% SL). Dorsal margin of head sloping from supraoccipital crest to snout; HL 30.3–39.7% SL (34.6% SL); head depth 50.3–75.1% HL (59.4 HL); eye large, orbit diameter 20.9–33.0% HL (24.6% HL), orbit with bony ridge extending over anterodorsal margin; interorbital ridge moderately wide, interorbital area slightly convex, interorbital width 21.6–32.9% HL (25.9% HL); suborbital depth 2.5–8.5% HL (5.6% HL); snout length 17.2–27.4% HL (21.3% HL), nostrils anterior to central point of orbit, anterior nostril with spatulate flap extending posteriorly dorsal to posterior nostril and surpassing vertical bisecting posterior nostril when de-

Table 3

Mean, minimum, maximum, and standard deviation (SD) values of meristics and linear morphometrics for *Sebastes mystinus* (blue rockfish; $n=68$) and *S. diaconus* (deacon rockfish; $n=58$) examined for this study. Values for holotype of *S. diaconus*, new species, CAS 236653, and lectotype of *S. mystinus*, USNM 27085, are also provided. Standard length in millimeters. Linear morphometrics are given in proportions to standard length or head length for cephalic measurements (orbit length–symphyseal knob length).

	<i>S. mystinus</i>					<i>S. diaconus</i>				
	Lectotype	Mean	Min	Max	SD	Holotype	Mean	Min	Max	SD
Dorsal-fin spines	13	13	12	15	0.4	13	13	12	13	0.2
Dorsal-fin rays	15	15	13	17	0.7	16	16	14	17	0.8
Anal-fin spines	3	3	3	3	0.0	3	3	3	3	0.0
Anal-fin rays	9	9	8	10	0.5	9	9	8	9	0.4
Left total pectoral-fin rays	18	18	16	18	0.4	17	18	16	18	0.5
Right total pectoral-fin rays	17	18	17	19	0.6	18	18	17	18	0.5
Left unbranched pectoral-fin rays	10	10	9	12	0.4	10	10	9	10	0.3
Right unbranched pectoral-fin rays	10	10	9	11	0.4	10	10	10	10	0.3
Lateral-line pores	48	48	42	52	2.3	49	45	41	51	2.7
Scales in mid-lateral series	57	58	54	68	3.2	65	62	56	68	2.8
Anterior gill rakers	34	33	30	39	1.7	34	33	28	35	1.7
Posterior gill rakers	22	25	21	27	1.3	25	22	21	26	1.3
Dorsal procurent caudal-fin rays	12	12	11	12	0.4	11	12	11	13	0.7
Ventral procurent caudal-fin rays	12	11	11	12	0.5	12	11	11	12	0.5
Dorsal main caudal-fin rays	8	8	8	8	0.0	8	8	8	8	0.0
Ventral main dorsal-fin rays	8	8	8	8	0.0	8	8	8	8	0.0
Vertebrae	26	26	26	27	0.3	27	26	26	27	0.3
Standard length	249.6	164.2	45.7	324.0	80.6	260.0	181.3	48.2	330.0	73.8
Head length	34.7	33.7	29.9	36.4	1.5	35.3	34.5	30.3	39.7	1.9
Orbit length	7.3	24.6	17.3	30.4	2.7	7.5	24.6	20.9	33.0	2.7
Snout length	6.8	20.9	16.5	28.2	2.5	8.4	21.3	17.2	27.4	2.7
Interorbital width	9.7	26.2	18.1	32.0	3.3	9.9	26.0	21.6	32.9	2.0
Suborbital depth	2.4	6.0	4.0	8.9	0.9	2.6	5.6	2.5	8.5	1.2
Head depth	20.8	61.3	53.8	73.8	4.4	19.7	59.8	40.4	76.9	7.5
Upper jaw length	14.0	41.8	36.5	46.8	2.3	13.7	40.9	36.2	48.1	2.5
Lower jaw length	10.4	31.9	27.3	37.0	2.1	12.8	32.3	27.3	40.9	3.1
First gill arch length	14.7	43.3	30.6	53.5	4.0	14.0	42.3	32.3	49.0	3.5
Symphyseal knob length	1.7	4.5	2.6	5.7	0.7	2.0	5.5	4.0	7.0	0.7
Predorsal fin length	32.2	32.4	28.6	40.3	2.3	35.3	33.5	28.9	42.4	2.1
Prepelvic fin length	38.6	39.6	34.1	48.3	2.8	38.6	39.9	33.3	47.8	2.5
Preanal fin length	77.2	70.7	64.4	77.2	2.5	72.7	70.2	64.0	76.7	2.7
Depth at dorsal fin origin	36.2	34.4	28.4	39.8	2.0	34.2	33.5	24.7	36.8	2.0
Depth at pelvic fin origin	37.1	35.3	28.8	40.8	2.1	34.5	34.4	25.4	39.5	2.3
Depth at anal fin origin	31.7	29.8	23.0	34.1	2.2	32.5	29.7	22.0	34.8	2.3
Dorsal-fin spine I length	5.1	4.7	3.4	6.1	0.6	4.9	4.7	2.7	6.2	0.6
Dorsal-fin spine IV length	12.4	11.6	8.7	13.8	1.0	12.9	12.0	9.9	13.4	0.9
Spinous dorsal-fin base length	36.7	37.5	31.2	41.4	2.3	38.3	36.9	32.1	41.0	2.2
Soft rayed dorsal-fin base length	23.0	24.1	20.5	29.4	1.6	22.9	24.1	20.8	27.6	1.5
Pectoral-fin base depth	11.0	10.3	8.4	11.7	0.8	10.3	10.0	7.8	11.4	0.7
Pectoral fin length	30.5	29.3	25.6	32.7	1.8	29.2	28.8	23.7	32.0	1.7
Pelvic-fin ray length	20.6	20.2	16.3	23.4	1.7	22.1	19.8	16.8	22.4	1.3
Pelvic-fin spine length	13.8	12.7	8.9	15.6	1.3	12.9	12.4	9.3	14.7	1.2
Anal-fin base length	16.4	16.9	14.7	19.8	1.1	18.2	17.0	14.6	19.7	1.2
Anal-fin spine I length	4.5	4.5	1.8	6.7	1.0	6.2	4.8	3.3	6.7	0.8
Anal-fin spine II length	8.3	9.7	6.4	13.2	1.8	11.4	10.2	7.3	13.6	1.4
Anal-fin spine III length	11.8	10.7	7.5	13.8	1.4	10.9	11.0	6.7	14.2	1.4
Dorsal fin origin to anal fin origin	57.8	51.1	42.1	60.1	3.1	54.0	50.4	44.6	55.0	6.1
Caudal peduncle depth	11.1	10.6	8.6	12.5	0.9	11.0	10.5	8.9	12.7	0.7
Caudal peduncle dorsal length	10.8	11.8	8.6	15.3	1.6	8.2	12.3	8.2	16.3	1.7
Caudal peduncle ventral length	19.2	18.0	14.1	21.4	1.6	18.9	17.8	14.5	23.1	1.7

pressed, posterior nostril larger than anterior and without flap; cranial spines mostly absent with the exception of moderately weak nasal spines. Mouth terminal and moderately sized with posterior margin of maxilla extending to vertical through mid-pupil, posterior margin of maxilla slightly rounded, upper and lower jaw forming 30–35° angle to central axis of body when closed; upper jaw length 36.2–48.1% HL (40.9% HL), premaxilla with patches of minute conical teeth near symphysis transitioning into 2 then 3 rows of teeth along posterolateral portion, palatine and vomer covered in small conical teeth; lower jaw extending anteriorly slightly beyond upper jaw, protrusion becoming more distinct with growth, lower jaw length 27.4–40.9% HL (32.3% HL), mandibular pores minute or absent, mandible with 2–3 rows of minute conical teeth; tongue smooth; symphyseal knob pronounced and blunt (Fig. 7A), knob length 4.0–7.0% HL (5.5% HL); gill arch length 32.3–46.0% HL (42.3% HL); dorsal margin of opercular flap extending posteroventrally at a 25° angle to horizontal midline of the body, posterior margin of opercular flap straight, curving ventrally; opercular spines 2, dorsal spine stronger than ventral; preopercular spines 5, of which dorsal 3 are moderately developed, third largest, fourth weak and fifth very weak.

Predorsal length 28.9–42.4% SL (33.5% SL); prepelvic length 33.3–47.8% SL (39.9% SL); preanal length 64.0–77.7% SL (70.3% SL). Dorsal-fin origin above posterior extent of opercular flap, dorsal-fin base length 55.0–68.2% SL (60.9% SL), spinous dorsal-fin base 32.1–41.0% SL (36.9% SL), first dorsal-fin spine 2.7–6.2% SL (4.7% SL), first spine shortest and subsequent spines rapidly increasing in height, longest dorsal-fin spine (IV) 9.9–13.4% SL (12.0% SL), spines IV–VII of approximately equal length with subsequent spines decreasing in size, 1 spine present at origin of rayed portion of dorsal fin, rayed dorsal-fin base 20.8–27.6% SL (24.0% SL), anterior rays longest and decreasing in size posteriorly, fin sloping posteroventrally and straight, not curved. Anal-fin margin perpendicular to body axis, posterior tips of rays forming nearly vertical line, anal-fin base 14.6–19.7% SL (17.0% SL), anterior anal-fin rays longest and decreasing in length posteriorly, anal-fin spine I length 3.3–6.7% SL (4.9% SL), anal-fin spine II length 7.3–13.6% SL (10.2% SL), thicker than others, anal-fin spine III length, usually longest, 6.7–14.2% SL (11.0% SL); pectoral-fin length 23.8–32.1% SL (28.8% SL), pectoral-fin base height 7.8–11.4% SL (10.0% SL), branched rays present on dorsal half of fin with transition to unbranched rays occurring 1 or 2 rays above the midline of the fin; pelvic-fin length 15.8–22.4% SL (19.7% SL), pelvic-fin rays decreasing in size from origin, posterior margin of pelvic fins slightly rounded; pelvic-fin spine length 9.3–14.7% SL (12.3% SL); caudal-peduncle depth 8.9–

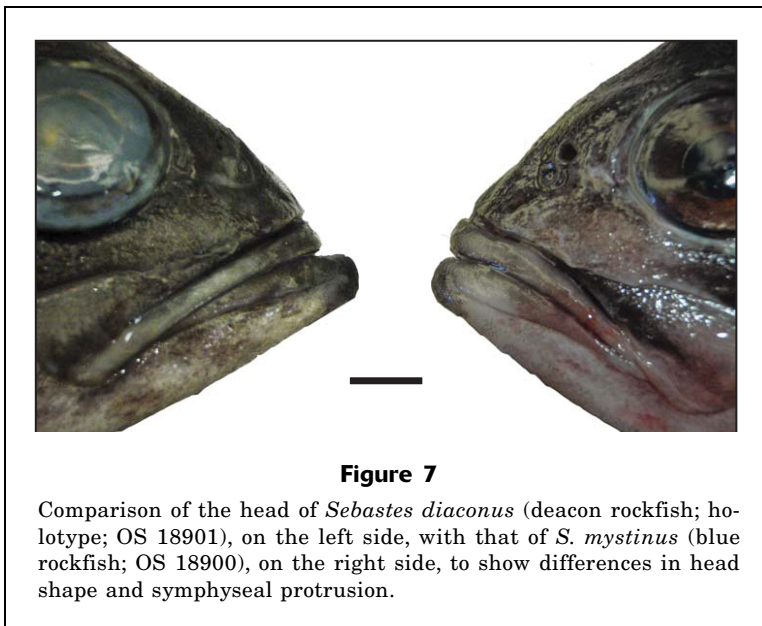


Figure 7

Comparison of the head of *Sebastes diaconus* (deacon rockfish; holotype; OS 18901), on the left side, with that of *S. mystinus* (blue rockfish; OS 18900), on the right side, to show differences in head shape and symphyseal protrusion.

12.7% SL (10.5% SL), dorsal caudal-peduncle length 8.2–16.3% SL (12.3% SL); ventral caudal-peduncle length 14.5–23.1% SL (17.8% SL), caudal fin weakly emarginate, length not recorded because of extensive damage in many specimens.

Body covered in rough ctenoid scales; head entirely scaled, scales above dorsal opercular opening origin unorganized and very small, scales organized into loose rows on preopercle and opercle, scales on snout, premaxilla, maxilla and lower jaw minute and unorganized. Trunk scales moderately large, flanked by many small accessory scales, especially along posterior margins; lateral-line pores conspicuous and forming distinct line approximately one-quarter of body depth below dorsal margin of body, curving ventrally to reach midline of body axis at vertical through dorsal-fin insertion. Fins completely scaled, with exception of membranes between dorsal spines and posterior regions of unbranched pectoral-fin rays.

Coloration of live specimens (Figs. 1A and 8A) Body overall dark brown to blue-gray, becoming lighter posteriorly, ventrum white to light gray; small speckles covering sides of the body but not forming large blotches, pattern more evident in mature specimens. Juveniles (<100 mm SL) generally darker than adults, speckles indistinct or absent on trunk, and difficult to distinguish from other dark-bodied species. Head with 2 dark oblique bars extending posteriorly below orbit, 1 or 2 additional dark bars over cranium and opercular flap. Dorsal-fin membrane dark, lacking spots; caudal and anal fins uniformly blackish blue, thin light or unpigmented band on posterior margin of caudal fin; pelvic fins light with blue tips on rays, pelvic-fin spine white; pectoral fins dark blue dorsally, with light coloration on unbranched rays and ventral half of pectoral fins. Peritoneum dark, usually black to gray, typically

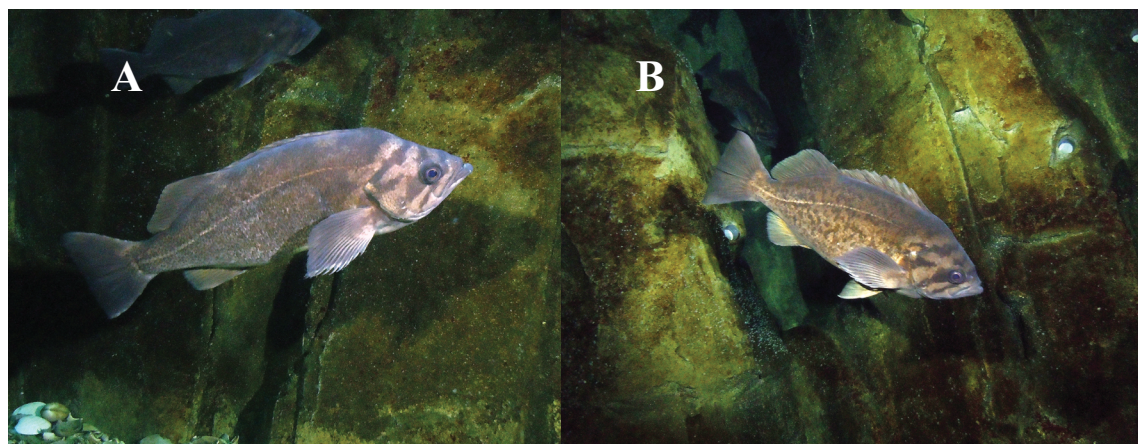


Figure 8

Photographs of live (A) *Sebastes diaconus* (deacon rockfish) and (B) *S. mystinus* (blue rockfish) in the Oregon Coast Aquarium, Newport, Oregon.

lighter in large specimens; stomach and other internal organs pale beige to grayish.

Coloration of preserved specimens (Fig. 1C) Shortly after death and during the process of preservation, trunk color becomes dull, dark gray to brown and the speckling pattern becomes less apparent; ventrum light brown to cream. Dorsal cranial bands fade and become indistinct, and 2 bands below orbit fade in color to match rest of body.

Etymology

Sebastes diaconus is derived from the Latinized ancient Greek δῆκονος, the name for an acolyte or assistant to a priest. This name complements the species name of *S. mystinus*, which was intended to mean “priest” (Jordan and Evermann, 1898). This name highlights the similarity between the 2 species and the previous lack of differentiation.

Distribution

Sebastes diaconus is distributed from Vancouver Island in British Columbia to a southernmost record in Morro Bay, California (between 35°N and 48°N). All specimens with records of their collection depths were taken at depths of 8–50 m. The holotype and paratypes were collected from the Pacific Ocean off the coast of central Oregon (Fig. 9). Very little material was available from British Columbia and Alaska; therefore, the northern extent of the range remains unclear (Fig. 9). One poorly preserved specimen, USNM 54440, collected during an *Albatross* survey in 1897 off Killisnoo Island in southeastern Alaska may be a specimen of *S. diaconus*. However, it could also

represent *S. ciliatus* and is excluded from the type and examined material. All other putative specimens of *S. mystinus* from Alaska that we examined had been misidentified and are mostly *S. ciliatus*. On the basis of this and previous work (Cope, 2004; Burford and Bernardi, 2008; Burford, 2009), *S. diaconus* appears to be much more abundant at latitudes higher than northern California.

Sebastes mystinus (Jordan and Gilbert, 1881)

English common name: blue rockfish

Figures 1, B and D, 2–6, 7B, 8B, 9, 10, and 11; Tables 1–3.

Sebastes variabilis (Pallas, 1814): Ayres, 1854:7 (specimens from California considered similar to but likely not that described in Pallas [1814]); Jordan and Gilbert, 1881:70.

Sebastichthys melanops (Girard, 1856): Jordan and Gilbert, 1880b:289.

Sebastes melanops (Girard, 1856): Ayres, 1862:216 (in part, (not in fig. 66, but elsewhere in description); Jordan and Gilbert, 1881:70.

Sebastichthys mystinus Jordan and Gilbert, 1881 (for 1880b):455 (type localities: San Francisco and Monterey, California; described from 11 specimens).

Sebastes mystinus (Jordan and Gilbert, 1881): Jordan and Gilbert (1882):659 (new combination).

Primospina mystinus (Jordan and Gilbert, 1881): Eigenmann and Beeson, 1893:669 (new combination).

Sebastosomus mystinus (Jordan and Gilbert, 1881): Jordan and J. Z. Gilbert, 1919:51 (new combination); Jordan and J. Z. Gilbert, 1920:32 (with mention that Jordan was inclined to elevate subgenus, but unclear if this decision was published); Jordan et al., 1930:365 (last reference to combination).

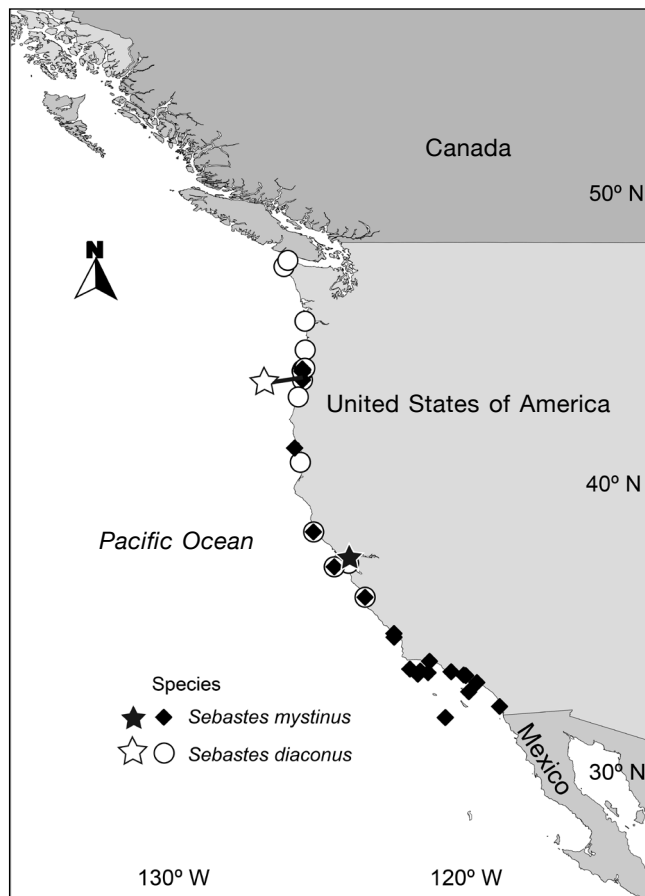


Figure 9

Distribution map of individuals of *Sebastes diaconus* (deacon rockfish; open circle; white star corresponding to holotype [OS 18901] locality) and *S. mystinus* (blue rockfish; black diamond; black star corresponding to lectotype [USNM 27085] locality) examined in this study.

Sebastes mystinus (Jordan and Gilbert, 1881): Hart, 1973:429; Eschmeyer and Herald, 1983:144; Orr et al., 2000:27; Love et al., 2002:215 (in part); Love, 2011:250–251 (in part).

Lectotype

USNM 27085, 1, 249 mm SL, off San Francisco, CA, 1880, D. S. Jordan.

Paralectotypes

MNHN A-3286 (ex-USNM 27085), 1, 185 mm SL, off San Francisco, CA, 1880, D. S. Jordan; MSNG 8327 (ex-USNM 26791), 1, 250 mm SL, off Monterey, CA, 1880, D. S. Jordan; MTD F 174 (ex-USNM 27085), 1, off San Francisco, CA, 1880, D. S. Jordan, desiccated specimen; RMNH-PISC 11530 (ex-USNM 26971), 1, 198 mm SL, off Monterey, CA, 1880, D. S. Jordan; USNM 26971, 212

mm SL, off Monterey, CA, 1880, D. S. Jordan; USNM 427237 (ex-USNM 27085), 1, 201 mm SL, off San Francisco, CA, 1880, D. S. Jordan; ZMUC P791064 (ex-USNM 27031), 1, 180 mm SL, off Monterey, CA, 1880, D. S. Jordan.

Additional material

CAS 13711, 1, 170 mm SL, off Southern California, east of Bishop Rock, 32°27'N, 119°7'59.10"W, 27.4 m depth, 28 July 1889, C. H. Eigenmann; CAS 14806, 4, 101–116 mm SL, Monterey Bay, Coast Guard Jetty, CA distance offshore 6.1–9.1 m, *Macrocystis* bed, 4.6–13.7 m depth, 14 August 1972, Behrens et al.; CAS 15439, 1, 193 mm SL, southern end of Santa Monica Bay, just north of Rocky Point, Palos Verdes Peninsula, CA, 24.4–27.4 m depth, 15 September 1972, E. W. Iverson; CAS 15440, 5, 150–182 mm SL, Santa Rosa Island, off Fraser Point, CA, 9.1–82.3 m, 21 September 1972, E. W. Iverson; CAS 234207, 1, 131 mm SL, off Santa Cruz Island, CA, 29 August 1954, E. Hunter; CAS 25884, 2, 64–70 mm SL, Pacific Grove, Monterey, CA, 6 October 1953, W. I. Follett; CAS 26469, 4 of 7, 130–176 mm SL, Souza Rock, Morro Bay, CA, 9 June 1953, G. D. Hanna; CAS 27719, 2, 50–101 mm SL, Point Arena, Arena Cove, CA, 38°54'56"N, 123°43'26"W, 9.1–12.2 m depth, 15 August 1972, R. Lea et al.; CAS 30262, 1, 265 mm SL, Santa Catalina Island, rocky bank off Avalon, CA, 6 June 1973, A. Loukashkin; SU 10149, 1, 273 mm SL, Cortez Bank, Baja California, Mexico, *Albatross* survey, U.S. Fish Commission; SU 15104, 1 of 10, 118 mm SL, Pacific Grove, pier at far end of city beach, California, 2 August 1948, E. Walker, C. Limbaugh, and A. Flechsig; SU 48885, 1, 76 mm SL, Morro Bay, beach just beyond PG&E intake on road to Morro Rock, San Luis Obispo, CA, 35°22'15"N, 120°55'20"W, 30 October 1995, B. W. Walker, UCLA party and San Simeon party; LACM 6607.001, 8, 65–77 mm SL, Leo Carillo State Park, Los Angeles, CA, 6 December 1964, E. S. Hobson and party; LACM 9482.002, 5 of 10, 136–234 mm SL, 8.0–9.7 km, north-northwest of San Miguel Island, CA, 6 December 1962, B. Wood; LACM 31864.024, 5, 88–100 mm SL, El Segundo, Los Angeles, CA, 25 March 1971, C. C. Swift and R. J. Lavenberg; LACM 35705.012, 1, 95 mm SL, off Huntington Beach power plant, CA, 11 June 1971, RV *Searcher*; LACM 47933.002, 241 mm SL, northeast end, 3.2 km offshore, Santa Rosa Island, CA, 5 June 1949, J. Fitch; LACM 47933.003, 46 mm SL, northeast end ~3.2 km offshore, Santa Rosa Island, CA, 5 June 1949, J. Fitch; LACM 48124.002, 2, 68–71 mm SL, point at Arguello Boat Station, Santa Barbara, CA, 22 October 1949, B. W. Walker and party; LACM 50157.002, 1, 56 mm SL, about 3.2 km north of San Simeon and 4.0 km south light at Coast Guard station, CA, 16 November 1999, B. W. Walker and class; OS 2618, 1, 222 mm SL, San Francisco Bay, CA, 15 May 1949, E. A. Brooks; OS 18881, 1, 257 mm SL, 1.4 km west of Tokatee Kloochman State Natural Site, OR, 44°12'26.28"N, 124°8'2.04"W,

19.2 m depth, 24 April 2012, D. W. Wagman and T. N. Frierson; OS 18886, 3, 223–300 mm SL, 1.3 km west of southern end of Lost Creek State Park, OR, 44°32′35.95″N, 124°5′33.61″W, 12.8 m depth, 24 April 2012, D. W. Wagman and T. N. Frierson; OS 18887, 3, 225–267 mm SL, 1.3 km west of south end of Lost Creek State Park, OR, 44°32′36.10″N, 124°5′33.40″W, 15.5 m depth, 20 April 2012, D. W. Wagman and T. N. Frierson; OS 18891, 3, 275–321 mm SL, 1.2 km west of north end of Lost Creek State Park, OR, 44°33′26.93″N, 124°5′18.17″W, 14.1 m depth, 20 April 2012, D. W. Wagman and T. N. Frierson; OS 18892, 1, 312 mm SL, 1.4 km west of north end of Lost Creek State Park, OR, 44°33′34.63″N, 124°5′45.02″W, 14.5 m depth, 8 May 2012, D. W. Wagman and T. N. Frierson; OS 18894, 2, 215–234 mm SL, 1.7 km north-west of Lost Creek State Park, OR, 44°33′51.12″N, 124°5′42.18″W, 14.3 m depth, 8 May 2012, D. W. Wagman and T. N. Frierson; OS 18896, 1, 295 mm SL, 1.5 km west of Lost Creek State Park, OR, 44°33′13.26″N, 124°5′38.54″W, 13.5 m depth, 8 May 2012, D. W. Wagman and T. N. Frierson; OS 18898, 1, 208 mm SL, 2.8 km west off south end of South Beach State Park, OR, 44°33′38.83″N, 124°6′36.47″W, 28.9 m depth, 15 May 2012, D. W. Wagman and T. N. Frierson; OS 18899, 1, 227 mm SL, 3.3 km west of south end of South Beach State Park, OR, 44°35′42.79″N, 124°6′35.82″W, 28.9 m depth, 15 May 2012, D. W. Wagman and T. N. Frierson OS 18900, 267 mm SL, 1.8 km west of Seal Rock, OR, 44°29′49.38″N, 124°6′30.48″W, 20.9 m depth, 20 April 2012, D. W. Wagman and T. N. Frierson; USNM 26947, 1, 163 mm SL, Santa Barbara, CA, 1880, D. S. Jordan; USNM 47154, 1, 270 mm SL, Cortez Banks, off Southern California, 37 m depth, 1889, *Albatross* expedition; USNM 63545, 1, 119 mm SL, Sausalito, CA, date unknown, *Albatross*; USNM 104771, 1, 161 mm SL, Point Pinos, Monterey, CA, 5 February 1923, C. L. Hubbs. UW 114028, 1, 210 mm SL, Scripps Canyon, La Jolla, CA, 32°49′59.88″N, 117°15′0″W, 14 November 2000, collector unknown.

Designation of lectotype

The original description by Jordan and Gilbert (1881) was published well before the establishment of the convention of holotype and paratypes designations. However, shortly after the original description, Jordan and Jouy (1881) published a listing of type material at the USNM for *Sebastichthys mystinus*. The type material listed includes USNM 26971 and 27031 from Monterey, California, and USNM 27085 from San Francisco, California, without any indication of the number of specimens in each lot. However, 10 syntypes are known to exist, including 5 in USNM: 26971 (1), 27031 (1), 27085 (3, of which 1 is an osteological preparation). In addition, there is 1 in each of 5 collections in Europe: MNHN A-3286 (ex-USNM 27085), MSNG 8327 (ex-USNM 26971), MTD F 174 (ex-USNM 27085, specimen desiccated), RMNH-PISC 11530 (ex-USNM 26971), and ZMUC P791064 (ex-USNM

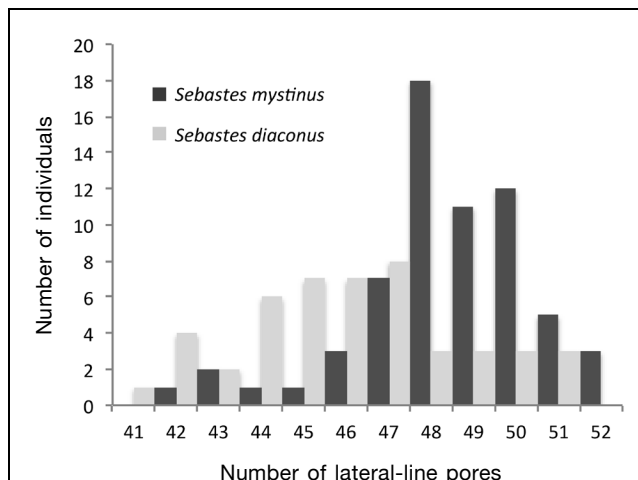


Figure 10

Histogram of lateral-line pore counts for specimens of *Sebastes diaconus* (deacon rockfish; $n=47$; gray bars) and *S. mystinus* (blue rockfish; $n=68$; black bars) examined in this study.

27031). An eleventh syntype was sent to Philadelphia (ANSP 12119, ex-USNM 27085), but it is currently missing (Böhlke, 1984; Sabaj Peréz³). USNM 27085 was selected as the lectotype of *S. mystinus* because it is in the best condition of the original type material and has obvious blotched pigmentation (Fig. 11). One of the 10 extant syntypes of *S. mystinus*, USNM 27031, does not conform to the description of *S. mystinus*, clearly does not match the rest of the type series or the published illustration of this specimen (Jordan and Evermann, 1900: pl. 270, fig. 657; listed as fig. 656 in the index), and is a different species of *Sebastes* (see the *Remarks* section). We designate the remaining specimens in the syntype series, with the exceptions of the misidentified USNM 27031 and the missing ANSP 12119, as paralectotypes.

Diagnosis

A species of *Sebastes* differentiated from all congeners with the exceptions of *S. ciliatus*, *S. melanops*, and *S. diaconus* by possessing dark gray, blue, brown, or black body coloration, scales covering the mandible, and weak or absent head spination. *Sebastes mystinus* is distinguished from *S. ciliatus* and *S. melanops* by the maxilla not extending beyond the posterior margin of pupil when the mouth is closed. It is further distinguished from *S. ciliatus* by 4 bars of dark pigmentation extending across the head and nape versus an almost uniformly dark head coloration with 2 faint bars below orbit in *S. ciliatus*, 26–27 vertebrae versus

³ Sabaj Peréz, M. 2013. Personal commun. Department of Ichthyology, The Academy of Natural Sciences, Philadelphia, PA 19103.

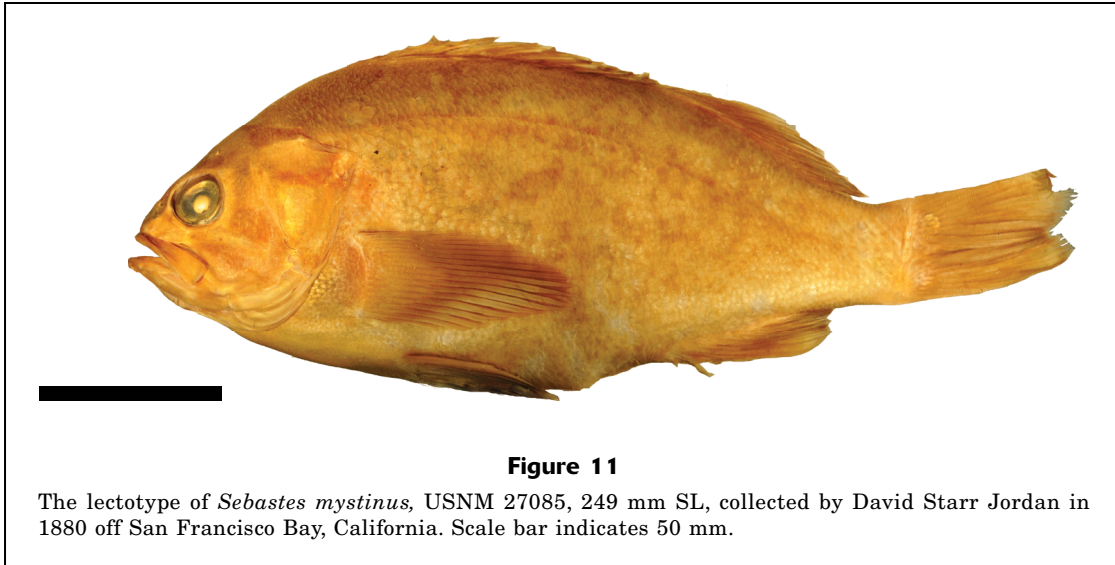


Figure 11

The lectotype of *Sebastes mystinus*, USNM 27085, 249 mm SL, collected by David Starr Jordan in 1880 off San Francisco Bay, California. Scale bar indicates 50 mm.

28–29 vertebrae in *S. ciliatus*, and a small or absent symphyseal knob versus a pronounced one. It is further distinguished from *S. melanops* by having a blue-gray trunk with large gray blotches, versus a darker black or gray trunk with irregular areas of dark pigmentation ranging from speckling to blotches in *S. melanops*, and by having dark dorsal-fin membranes without dark spots, versus the presence of such spots. *Sebastes mystinus* is distinguished from *S. diaconus* by a steel-blue to greenish-blue body coloration with large, distinct dark blotches versus a dark blue-brown to blue-gray body with a light, speckled pattern that characterizes *S. diaconus*. It is further distinguished from *S. diaconus* by the following set of character states in individuals over ~150 mm SL: ventral margin of head and ventrum generally rounded, giving the body a more ovoid appearance, versus the flat ventrum of *S. diaconus*; symphyseal knob short and not prominent (length of dentary symphysis 2.6–5.7% HL) versus well-developed (4.0–7.0% HL). Although these ranges overlap, symphyseal knob length differs diagnostically among specimens of equal size over 150 mm SL. This measurement can be diagnosed by reference to allometric plots (Fig. 6A).

Description

Description based on 68 specimens, 45.7–324.0 mm SL. Counts and measurements of lectotype and ranges, averages, and standard deviations for all specimens are provided in Table 3. Values in parentheses are modes for meristic counts and means of all specimens for morphometric ratios.

Dorsal-fin spines XXII to XXIV (XXIII) [1 with XXV], rays 13–17 (15); anal-fin spines III, rays 8–9, rarely 10 (9); pectoral-fin unbranched rays 9 or 10, rarely 11 (10), branched rays 7–9 (8), total pectoral rays 16–19 (18); pelvic-fin spines 1; pelvic-fin rays 5; total caudal-fin

rays 38–40 (40); dorsal segmented caudal rays 8; ventral segmented caudal rays 8; dorsal procurvent caudal rays 11–12 (12); ventral procurvent caudal rays 11–12 (11); total vertebrae 26, rarely 27; anterior gill rakers 30–39 (33); posterior gill rakers 21–27 (25); scales ctenoid; lateral-line pores 42–52 (48); scales in lateral series on midline 54–68 (58).

Body deep and ovoid; depth at pelvic-fin origin 28.8–40.8% SL (35.3% SL); depth at anal-fin origin 23.0–34.1% SL (29.7% SL); depth at dorsal-fin origin 28.4–39.8% SL (34.3% SL). Dorsal margin of head slightly rounded (Fig. 6B); head length 29.9–36.4% SL (33.6% SL); head depth 53.8–73.8% HL (61.5 HL); eye moderately large, orbit diameter 17.3–30.4% HL (24.6% HL), bony ridge extending over anterodorsal margin of orbit; interorbital ridge wide and convex, interorbital width 18.1–32.0% HL (26.3% HL); suborbital depth 4.0–8.9% HL (6.0% HL); snout length 16.5–28.2% HL (20.9% HL). Nostrils anterior of mid-orbit, anterior nostril circular with wide spatulate nostril flap that extends to posterior side of posterior nostril when depressed, posterior nostril ovoid and larger than anterior nostril, posterior nostril without flap; cranial spines usually absent except for weak nasal spines, additional weak head spines have been rarely reported (Love et al., 2002). Terminal mouth with moderate gape, posterior tip of maxilla extending at least to vertical through center of orbit and at maximum to vertical through posterior margin of pupil, posterior margin of maxilla flat to minimally rounded. Jaws when closed forming dorsally slanted 30° angle to midline of body; upper jaw length 36.5–46.8% HL (41.8% HL), premaxilla with 2 broad patches of small unorganized conical teeth near symphysis, teeth forming 2–3 rows that terminate one-third premaxilla length before posterior tip of premaxilla, palatine and vomer with patches of minute conical teeth; anterior tip of lower jaw level with or slightly anterior to upper jaw when mouth closed, not exaggerated in larger

specimens, lower jaw length 27.3–37.0% HL (31.8% HL), mandible with patches of 5 or 6 rows of teeth near symphysis that become 3 rows of minute conical teeth away from symphysis, mandibular pores weak or absent, tongue smooth; symphyseal knob generally weak to absent, more pronounced in larger specimens, but not exaggerated, symphyseal knob length 2.6–5.9% HL (4.6% HL); gill arch length 30.6–53.5% HL (43.4% HL). Dorsal margin of opercular flap extends at posteroventral 18–20° angle with body midline, posterior margin of opercular flap straight, sloping at 65° anteroventral angle to body midline, curving anteriorly near ventral extreme; opercular spines 2, both weakly protruding from skin, dorsal spine slightly stronger than ventral spine; preopercular spines 5, dorsal 4 spines moderately developed, fifth spine small and weak.

Predorsal length 28.6–40.3% SL (32.4% SL); prepelvic length 34.1–48.3% SL (39.6% SL); preanal length 64.4–76.1% SL (70.6% SL). Origin of dorsal fin slightly anterior to posterior tip of opercular flap, dorsal-fin base length 55.3–67.4% SL (61.6% SL), spinous dorsal-fin base 31.2–41.2% SL (37.5% SL), spinous portion of dorsal fin slightly rounded, highest in middle, dorsal-fin spine I 3.4–6.1% SL (4.7% SL), first dorsal spine shortest, subsequent spines much longer, longest dorsal-fin spine (IV) 8.7–13.8% SL (11.6% SL), dorsal spines IV–VII roughly the same length, with posterior spines decreasing in length, 1 spine at origin of rayed section of dorsal fin, rayed dorsal-fin base 20.5–29.4% SL (24.1% SL), dorsal-fin rays decreasing in size posteriorly forming straight sloping edge with a slightly curved anterior portion; anal-fin base 14.7–19.8% SL (16.9% SL), anal-fin spine I length 2.6–6.7% SL (4.5% SL), anal-fin spine II length 6.4–13.2% SL (9.7% SL), anal-fin spine III length, usually the longest, 7.5–13.8% SL (10.7% SL), anal-fin rays decrease in size posteriorly, posterior tips of rays form line nearly perpendicular to body axis, not curved; pectoral-fin length 25.6–32.7% SL (29.2% SL), pectoral-fin base height 8.4–11.7% SL (10.3% SL), pectoral-fin rays on dorsal half of fin branched, ventral 9–10 rays unbranched, rays thick and cylindrical; pelvic-fin length 16.3–23.4% SL (20.1% SL), lateralmost pelvic-fin ray longest, rays decreasing in size medially, posterior margin of fin straight, pelvic-fin spine length 8.9–15.6% SL (12.6% SL); caudal-peduncle depth 8.6–12.5% SL (10.6% SL), dorsal caudal-peduncle length 8.6–15.3% SL (11.8% SL); ventral caudal-peduncle length 14.1–21.4% SL (17.9% SL), caudal fin broad, weakly emarginate.

Rough scales with many small ctenii covering most of body; head, including jaws, completely scaled, scales on cranium between supraoccipital crest and snout minute and unorganized, these scales also cover jaws, circumorbital area, and region ventral to orbit; preopercle and opercle covered in loosely organized rows of larger scales, posteriorly flanked by accessory scales. Scales on trunk moderate to large, largest scales near midline of body, most trunk scales also posteriorly flanked by unorganized accessory scales; lateral-line pores not associated one-to-one with scales, forming a

slightly arched line along the dorsal third of the trunk originating at the dorsal insertion of opercular flap, curving to central midline of body at vertical through dorsal-fin insertion and terminating at caudal-fin base. Fins almost entirely scaled except for membranes of spinous dorsal and anal fins and posterior portions of the unbranched pectoral rays.

Coloration of live specimens (Figs. 1B and 8B) Overall body coloration somewhat variable, ranging from steel blue to greenish blue; ventrum white; sides of body with large, dark, angular blotches and no speckles; blotches easily discernible in larger juveniles (>100 mm SL) and mature adults; smaller juveniles generally solid brown-blue without distinct pattern of blotches. Head with 2 posteroventrally oriented dark bars, dorsal bar originating from orbit and extending to ventral margin of opercle, ventral bar running through orbit and over snout to terminate on ventral margin of opercular flap. One or 2 additional dark bars across dorsal surface of head behind orbit, terminating on opercular flap. Spinous dorsal-fin membrane completely dark and without spots, dorsal and caudal fin uniform dark blue to black, thin unpigmented strip on distal margin of caudal fin; anal fin slightly lighter, gray-blue to dark gray; pelvic fins light gray with blue tips, spine white to light gray; pectoral fins mostly dark blue-black, distal half of unbranched pectoral-fin rays light gray to white. Peritoneum usually black to dark gray, sometimes light in large specimens; stomach and other internal organs pale gray.

Coloration of preserved specimens (Figs. 1D and 1I) After death and during process of preservation, body pattern becomes less distinct and overall color fades to dark blue-brown; blotched pattern still visible on specimens through at least first 30 years of preservation. Blotches absent in some long-preserved specimens; however, this absence may reflect variation in preservation technique or exposure to light. Ventrum cream to light brown, dorsal and caudal fin dark blue-black, anal fin dark gray to dark blue-black, pelvic fin light with black tips, pectoral fins mostly brown-black, but distal half of unbranched rays white. Bars on head fade slightly, but remain dark and distinct; orbit cloudy white-blue.

Etymology

The species name in *Sebastes mystinus* is an adjective derived from the Latinized form of the ancient Greek word μύστης, which means initiated one or mystic (Hollmann⁴), although interpreted as “priest” (Jordan and Evermann, 1898). It was selected as the specific epithet because 19th century fishermen of Monterey, California, called the fish the “pêche prêtre” (translated as “priest-fish” by Goode, 1884) because of its overall

⁴ Hollmann, A. 2015. Personal commun. Department of Classics, Univ. Wash., Seattle, WA 98195.

dark coloration and its light band between the head bars that resembles a clerical collar (Goode, 1884; Jordan and Evermann, 1898).

Distribution

The true range of *S. mystinus* extends from central Oregon to northern Baja California (specimens examined from 32.5°N to 44.5°N), with the highest concentration of the species occurring off the coast of central to southern California (Fig. 9). Specimens examined were collected at depths of 0.5–30.0 m. Jordan and Gilbert (1881) originally described *S. mystinus* from specimens collected “off” San Francisco and Monterey, California. Subsequent observations cited the species as occurring from Baja California, Mexico, northward into British Columbia, and even Alaska (Love et al., 2002). However, it is apparent that all specimens examined from central Oregon northward into British Columbia are the new species, *S. diaconus*, and not *S. mystinus*. All purported specimens of *S. mystinus* from Alaskan waters that we examined belong to other congeners, primarily *S. ciliatus*.

Remarks

Ten of the 11 surviving syntypes of *S. mystinus* are clearly conspecific and match the original description by Jordan and Gilbert (1881). However, USNM 27031 is clearly not *S. mystinus* or *S. diaconus*, on the basis of substantial morphological differences. This specimen possesses an exceptionally long symphyseal knob and a maxilla extending almost to the posterior margin of the eye. In addition, its opercular spines are very well developed and much longer than observed in any *S. mystinus* or *S. diaconus* specimens. This specimen lacks distinctive pigmentation, such as head bars or blotching on the trunk; in fact it is entirely devoid of dark pigment. The other specimen originally in the same lot, ZMUC P791064 (ex-USNM 27031), is clearly recognizable as *S. mystinus* in that it lacks a symphyseal knob and bears a maxilla that extends posteriorly only to the vertical through the pupil of the eye. Additionally, it possesses faint head bars and blotching on the trunk.

Given the major differences between USNM 27031 and the remainder of the syntype series, it seems strange that Jordan and Gilbert (1881) would have conflated them. An illustration of USNM 27031 published by Jordan and Evermann (1900: pl. 270, fig. 657; also see Mecklenburg et al., 2002:360) may help explain the apparent lapse. The specimen currently designated as USNM 27031 does not correspond with the body shape or lower jaw shape of the illustration, and length of the specimen (402 mm TL, with significant caudal fin damage) far exceeds the measurement of 300 mm TL cited in the 1900 work. On the basis of the length of the specimen and the obvious shape difference, it is clear the current USNM 27031 is not the specimen originally designated by Jordan and Gilbert (1881) and illustrated by Jordan and Evermann (1900).

It is unclear how the current specimen designated as USNM 27301 came to possess this number, but a note attached to USNM 27031 states “1 located Nov. 21, 1946; some sent UZM Copenhagen 1881-7.” This note suggests that USNM 27031 was at one point lost and then relocated, presenting the possibility that the “relocated” specimen is not the original. The exact identification of USNM 27031 remains unclear. If it was originally dark-colored (now faded), it is most likely either an elongated specimen or a poorly preserved specimen of *S. melanops* or *S. ciliatus*. However, the lack of pigmentation could also indicate that this rockfish was originally light colored, a supposition supported by the fact that all other members of the syntype series retain some degree of dark coloration. If so, then the most likely species identification for this specimen is yellowtail rockfish *Sebastes flavidus* (Ayres, 1862). Either way, it undoubtedly does not represent *S. mystinus*, and we remove it from the paralectotype series.

Comparisons of *Sebastes mystinus*, *S. diaconus*, and similar congeners

Differentiation of the 2 species without the use of genetic techniques can be challenging, but the trunk coloration provides the most obvious difference between the 2 species. *Sebastes mystinus* is generally lighter colored, gray-blue to green-blue, and has a blotched pattern on the body, whereas *S. diaconus* is generally darker, blue to blue-brown, and has a distinct speckling pattern on the trunk (Fig. 1A). The difference in trunk pattern is apparent in juvenile specimens; however, smaller juveniles (<100 mm SL) of both species are almost entirely brown-gray with only subtle evidence of trunk markings. Coloration patterns are visible, but faint, in some preserved material making this diagnostic feature useful for historic specimens. *Sebastes diaconus* has a more pointed head and flat ventrum, as opposed to the generally rounded head and ventrum of *S. mystinus*. *Sebastes diaconus* specimens also have lower mean numbers of lateral-line pores (45 versus 48 in *S. mystinus*). Although the range of values overlaps almost completely (41–51 in *S. diaconus* versus 42–52, Fig. 10); only 16% of *S. diaconus* specimens possess more than 47 pored lateral-line scales versus 69% in *S. mystinus*, and the differences are statistically significant (Student’s *t*-test: $P=8.87 \times 10^{-6}$).

Specimens over 150 mm SL differ between species in the prominence and average length of the symphyseal knob, which measures 2.6–5.9% HL (4.6% HL) in *S. mystinus* and 4.0–7.0% HL (5.9% HL) in *S. diaconus* (Fig. 6A). Many juvenile specimens of both species lack a distinctly developed symphyseal knob. Lower jaw length (9.1–12.3% SL [10.4% SL] versus 9.3–14.0% SL [11.1% SL] in *S. diaconus*) and overall HL (29.9–36.3% SL [33.2% SL] versus 30.3–39.7% SL [34.7% SL] in *S. diaconus*) are also higher in *S. diaconus*. The lower jaw of *S. diaconus* extends farther beyond the anterior margin of the upper jaw than it does in *S. mystinus*, and this length may increase allometrically in *S. diacono-*

nus. However, this measurement differed only slightly significantly in a pairwise comparison (Student's *t*-test: $P=0.03$). The posteriormost corner of the opercle appears to be pointed in *S. diaconus* rather than rounded in *S. mystinus*; however, this shape difference is not apparent in juvenile specimens and may best be used as a field character rather than as a diagnostic. *Sebastes diaconus* specimens also possess, on average, longer first and second anal-fin spines: anal-fin spine I: 2.6–5.3% (3.9%) SL in *S. mystinus* versus 3.3–6.2% SL (4.6% SL) in *S. diaconus*, anal-fin spine II: 6.4–9.9% SL (8.3% SL) versus 7.3–12.2% SL (9.5% SL) in *S. diaconus*. The slopes of regressions for these spine lengths versus SL differ significantly (Figure 6, B and C).

Collection and dissection of specimens from off the Oregon coast between 2009 and 2014 indicate that ovary color of breeding females may also differ diagnostically (Hannah et al.⁵). Ovaries of breeding female *S. diaconus* examined immediately after capture were always pink-cream, whereas the ovaries of *S. mystinus* were always bright yellow. We did not observe this difference in the specimens used for genetic analysis; however, those specimens were not freshly deceased at the time of dissection.

Both *S. mystinus* and *S. diaconus* can be distinguished from the other potentially co-occurring dark-colored *Sebastes* species, such as *S. melanops* and *S. ciliatus*, on the basis of morphology and pigmentation. The color pattern of *S. diaconus* is very similar to that of some *S. melanops*; however, *S. melanops* tends to be darker black to brown with irregular gray blotches, mottling or speckling. The trunk coloration of *S. mystinus*, with large gray blotches, is generally lighter than that of *S. melanops*, and *S. melanops* is generally darker and more irregular in coloration. Additionally, both *S. diaconus* and *S. mystinus* have a smaller gape than that of *S. melanops*, with maxilla extending only to or just beyond the posterior margin of the pupil rather than beyond the posterior margin of the orbit. Some sources cite anal-fin shape to differentiate *S. mystinus* (and likely *S. diaconus*): a rounded anal fin versus a straight anal fin in *S. melanops* (Kramer and O'Connell, 1995). However, this character does not seem to be discrete because variation in fin shape between rounded and straight occurs in all 3 species.

Sebastes diaconus and *S. mystinus* are distinguished from *S. ciliatus* by having 4 bars of dark pigmentation across the head and nape, whereas *S. ciliatus* usually has uniform cephalic coloration (2 faint bars appear below the orbit occasionally) (Orr and Blackburn, 2004). As in *S. melanops*, the gape of *S. ciliatus* is larger than that of the other 2 species, with the maxilla extending to the posterior margin of the orbit. *Sebastes ciliatus*

is further distinguished from *S. mystinus* by having a more pronounced symphyseal knob, similar to that of *S. diaconus*. *Sebastes ciliatus* is known to occur mainly in Alaska and may range into northern British Columbia (Orr and Blackburn, 2004), whereas *S. mystinus* and *S. diaconus* occur farther south (all specimens of “*S. mystinus*” from Alaska examined were *S. ciliatus* or *S. variabilis*). Finally, *S. mystinus* and *S. diaconus* possess 26–27 vertebrae, and *S. ciliatus* has 28–29 vertebrae (Orr and Blackburn, 2004).

Discussion

Potential mechanisms for segregation

Although both pre- and postzygotic barriers may separate the 2 species, Burford et al. (2011a) suggested that a prezygotic explanation is more likely owing to the lack of hybrid individuals and strong Wahlund effect in areas of sympatry. Sympatric species of *Hexagrammos* in the northeastern Pacific show similar patterns of segregation (Crow et al., 2010). Prezygotic barriers may result generally from variable courtship behavior, incompatible reproductive morphological features, different reproductive timing, segregation of habitat type, or a combination of these factors. A least 3 of these factors are plausible in the specific case of *S. mystinus* and *S. diaconus*.

If differential courtship helps isolate these species, the development of species-specific characteristics at a size near, or preceding, early estimates of the length of first maturity (~150 mm SL in California populations of *S. mystinus*, Wyllie Echeverria, 1987; Love et al., 2002; Key et al.⁶; however, see Hannah et al.⁵) may facilitate prezygotic isolation by allowing breeding pairs to cue visually and tactilely on differences in body color (Fig. 1), in the size of the symphyseal knob (Fig. 6), or in the length of the lower jaw. In the only study to describe courtship behavior in *S. mystinus*, individuals were observed in Southern California (and, therefore, were clearly not *S. diaconus*) and during courtship the male was found to graze the snout of the female with its body (Helvey, 1982:fig. 3). The presence or absence of a moderately large symphyseal knob and longer lower jaw may act as an indication of species identity at this point. Comparison of the mating behavior of both species would be an important first step in exploring this hypothesis. Additionally, more recent work on both species in Oregon waters indicates larger lengths at first maturity for both species: around 260 mm fork length (FL) for *S. mystinus* and 270 mm FL for the other species (Hannah et al.⁵). The inclusion of more morphometric data from large individuals could elucidate further species-specific sexual characteristics.

⁵ Hannah, R. W., D. W. Wagman, and L. A. Kautzi. 2015. Cryptic speciation in the blue rockfish (*Sebastes mystinus*): age, growth and female maturity of the blue-sided rockfish, a newly identified species, from Oregon waters. Fish Div., Oregon Dep. Fish Wildl. Inf. Rep. 2015-01, 24 p. [Available at [website](#).]

⁶ Key, M., A. D. MacCall, J. Field, D. Aseltine-Neilson, and K. Lynn. 2007. The 2007 assessment of blue rockfish (*Sebastes mystinus*) in California, 112 p. Pacific Fishery Management Council, Portland, OR. [Available at [website](#).]

The differences between *S. mystinus* and *S. diaconus* in length of the anal-fin spines may imply additional mechanistic differences in internal fertilization. Helvey (1982) noted that at the probable point of insemination, male and female *S. mystinus* embrace with bodies in a C-shape position with their anal pores and anal fins tightly joined, indicating the use of anal-fin elements in copulation. The sexual dimorphism in anal-fin spine length in *S. melanops* (Wyllie Echeverria, 1986) and *S. mystinus* (Wyllie Echeverria, 1986; Lenarz and Wyllie Echeverria, 1991) further suggests a role for anal fin elements in internal fertilization among *Sebastes*. We did not observe sexual dimorphism in anal-fin spine lengths in this study, although sex was only verified on a subsample of specimens, and the use of anal-fin elements in sperm transfer has not been proven for these species. Therefore, the conjecture of differential reproductive morphological features remains speculative.

Differential reproductive timing may also play a role in prezygotic isolation of these 2 species. Hannah et al.⁵ observed ovary development for both species off central Oregon and identified a potential difference of a month in the timing of parturition with *S. diaconus* beginning in January and *S. mystinus* in February. However, sampling per month was uneven, and larger sample sizes may be necessary to confirm this difference.

Prezygotic isolation can also stem from habitat differences and particularly from differences among spawning sites. Although previous studies (Burford, 2009; Burford et al., 2011a, 2011b) found no clear evidence of differential habitat or depth preference between the 2 species, anecdotal evidence from fishermen and port samplers in central Oregon (Phillips⁷) indicates that adult *S. diaconus* are collected more frequently in deeper waters farther offshore than are adult *S. mystinus*, which are caught closer to shore in shallower waters. This variation in depth preference could explain the lack of type-1 (*S. diaconus*) adults found by Burford et al. (2011b) in nearshore surveys. Only new data on fisheries catches and intensive field observation will discern whether these species inhabit different physical environments.

Although previous research (Burford, 2011a) and evidence from this study support the possibility of segregation by means of prezygotic barriers, the possibility of segregation by postzygotic barriers, such as hybrid sterility or zygotic inviability, cannot be ruled out completely. Postzygotic barriers could be explored with controlled laboratory hybridization studies; however, breeding in captivity may not be realistic as rockfish mature slowly.

Implications for fisheries

The molecular analyses of Cope (2004) and of Burford and colleagues (Burford and Larson, 2007; Burford and

Bernardi, 2008; Burford, 2009; Burford et al., 2011a, 2011b), combined with our morphological results, indicate definitively that 2 types of blue rockfish differ sufficiently to merit recognition as distinct species. We concur with Burford et al.'s (2011a, 2011b) argument that fisheries management must recognize that distinction, because the 2 species may react differently to varying ocean conditions and may experience drastically different levels of fishing pressure. In the known area of sympatry (from Newport, Oregon, south through northern California), these 2 species hold substantial recreational importance and, to a lesser degree, commercial value. In northern California, blue rockfish (likely both species) are the most commonly caught species of rockfish by recreational fishermen and are the second largest recreational rockfish fishery after *S. melanops* in Oregon (Love et al., 2002). Central and southern California populations of blue rockfish (either *S. mystinus* or both species) have declined drastically and many of the fish currently being caught are juvenile, indicating stock depletion in these areas (Love et al., 2002). In response to the known decline, most of the fishery and life history research on blue rockfish has focused on southern California populations, likely *S. mystinus* (VenTresca et al., 1995; Laidig et al., 2003; Key et al.⁶), and very little appears to be known about *S. diaconus* from Oregon and Washington. Moreover, it is unknown whether fishing pressure in the zone of overlap affects 1 of the 2 species more than the other.

Our study provides fisheries managers the crucial diagnostic tool needed to answer these questions: namely, the characters that readily distinguish the adults of the 2 species, *S. mystinus* and *S. diaconus*, in the form of color pattern, size of the symphyseal knob and lower jaw, ventrum shape (rounded versus flat), and potentially ovary color. Although pelagic, young-of-year and early settled juveniles are more difficult to distinguish, as is the case with many young *Sebastes* (Love et al., 2002), genetic analysis or collection locality can help assign those individuals to these 2 species. Additional sampling and observational studies may also be able to elucidate ecological and habitat differences. Even with some gaps in our knowledge, formal recognition of these lineages as distinct species permits the development of proper management regimes for these important groundfishes along the Pacific coast of the United States.

Acknowledgments

We would like to thank D. Catania (CAS), M. Crag (ZMUC), G. Doria (MSNG), R. Fenney (LACM), K. Pearson Maslenikov (UW), T. Pietsch (UW), S. Raredon (USNM), P. Rask Møller (ZMUC), L. Rocha (CAS), R. de Ruiter (RMNH), M. Sabaj Peréz (ANSP), E. Taylor (UBC), and N. Vasset (MNH) for providing access specimens or images, M. Burford for providing genetic samples, S. S. Heppell, K. Hoekzema, T. Laidig, M. Love, D. Markle, J. Orr, and K. Schmidt for providing

⁷ Phillips, J. 2013. Personal commun. Hatfield Marine Science Center, Oregon State Univ., Newport, OR 97365.

feedback and support, our undergraduate helpers, A. Martin and E. Peterson, A. Hollmann (UW) for elucidating Ancient Greek etymology and for assisting with naming the new species, and the Oregon Coast Aquarium for access to exhibits. Support was provided by National Science Foundation Division of Biological Infrastructure NSF DBI 1057452 and U.S. Fish and Wildlife Service Federal Assistance Award OR F-186-R-9.

Literature cited

- An, H. S., J. Y. Park, M.-J. Kim, E. Y. Lee, and K. K. Kim.
2009. Isolation and characterization of microsatellite markers for the heavily exploited rockfish *Sebastes schlegeli*, and cross-species amplification in four related *Sebastes* spp. *Conserv. Genet.* 10:1969–1972. [Article](#)
- Ayres, W. O.
1854. Description of new fishes from California. *Proc. Calif. Acad. Nat. Sci.* 1:3–22.
1862. Descriptions of fishes believed to be new. *Proc. Calif. Acad. Nat. Sci.* 2:206–218.
- Bean, T. H.
1882. Notes on a collection of fishes made by Captain Henry E. Nichols, U.S.N., in British Columbia and southern Alaska, with descriptions of new species and a new genus (*Delolepis*). *Proc. U.S. Natl. Mus.* 4:463–474.
- Böhlke, E. B.
1984. Catalog of type specimens in the ichthyological collection of the Academy of Natural Sciences of Philadelphia. Special Publication 14, 216 p. *Acad. Nat. Sci. Phil., PA.*
- Burford, M. O.
2009. Demographic history, geographical distribution and reproductive isolation of distinct lineages of blue rockfish (*Sebastes mystinus*), a marine fish with a high dispersal potential. *J. Evol. Biol.* 22:1471–1486. [Article](#)
- Burford, M. O., and G. Bernardi.
2008. Incipient speciation within a subgenus of rockfish (*Sebastosomus*) provides evidence of recent radiations within an ancient species flock. *Mar. Biol.* 154:701–717. [Article](#)
- Burford, M. O., G. Bernardi, and M. H. Carr.
2011a. Analysis of individual year-classes of a marine fish reveals little evidence of first generation hybrids between cryptic species in sympatric regions. *Mar. Biol.* 158:1815–1827. [Article](#)
- Burford, M. O., M. H. Carr, and G. Bernardi.
2011b. Age-structured genetic analysis reveals temporal and geographic variation within and between two cryptic rockfish species. *Mar. Ecol. Prog. Ser.* 442:201–215. [Article](#)
- Burford, M. O., and R. J. Larson.
2007. Genetic heterogeneity in a single year-class from a panmictic population of adult blue rockfish (*Sebastes mystinus*). *Mar. Biol.* 151:451–465. [Article](#)
- Burnaby, T. P.
1966. Growth-invariant discriminant functions and generalized distances. *Biometrics* 22:96–110. [Article](#)
- Clemens, W. A., and G. V. Wilby.
1961. Fishes of the Pacific coast of Canada, 2nd ed. *Fish. Res. Board Can. Bull.* 68, 443 p.
- Cope, J. M.
2004. Population genetics and phylogeography of the blue rockfish (*Sebastes mystinus*) from Washington to California. *Can. J. Fish. Aquat. Sci.* 61:332–342. [Article](#)
- Crow, K. D., H. Munehara, and G. Bernardi
2010. Sympatric speciation in a genus of marine fishes. *Mol. Ecol.* 19:2089–2105. [Article](#)
- Earl, D. A., and B. M. vonHoldt.
2012. STRUCTURE HARVESTER: a website and program for visualizing STRUCTURE output and implementing the Evanno method. *Conserv. Genet. Res.* 4:359–361. [Article](#)
- Eigenmann, C. H., and C. H. Beeson.
1893. Preliminary note on the relationship of the species usually united under the generic name *Sebastodes*. *Am. Nat.* 27:668–671. [Available at [website](#).]
- Eschmeyer, W. N., E. S. Herald, and H. Hammann.
1983. A field guide to Pacific Coast fishes of North America, 336 p. Houghton Mifflin Co., Boston, MA.
- Falush, D., M. Stephens, and J. K. Pritchard.
2003. Inference of population structure using multilocus genotype data: linked loci and correlated allele frequencies. *Genetics* 164:1567–1587.
- Gharrett, A. J., A. P. Matala, E. L. Peterson, A. K. Gray, Z. Li, and J. Heifetz.
2005. Two genetically distinct forms of Rougheye rockfish (*Sebastes aleutianus*) are different species. *Trans. Am. Fish. Soc.* 134:242–260. [Article](#)
- Girard, C. F.
1856. Contributions to the ichthyology of the western coast of the United States, from specimens in the museum of the Smithsonian Institution. *Proc. Acad. Nat. Sci. Phila.* 8:131–137.
- Gomez-Uchida, D., E. A. Hoffman, W. R. Ardren, and M. A. Banks.
2003. Microsatellite markers for the heavily exploited canary (*Sebastes pinniger*) and other rockfish species. *Mol. Ecol. Notes* 3:387–389. [Article](#)
- Goode, G. B.
1884. The fisheries and fishery industries of the United States. Section I: natural history of useful aquatic animals, 895 p. Government Printing Office, Washington, D.C.
- Hammer, Ø., D. A. T. Harper, and P. D. Ryan.
2001. PAST: paleontological statistics software package for education and data analysis. *Palaeontologia Electronica* 4(1):1–9. [Available at [website](#).]
- Hart, J. L.
1973. Pacific fishes of Canada. *Fish. Res. Board Can. Bull.* 180, 740 p.
- Helvey, M.
1982. First observations of courtship behavior in rockfish, genus *Sebastes*. *Copeia* 1982:763–770. [Article](#)
- Hyde, J. R., and R. D. Vetter.
2007. The origin, evolution, and diversification of rockfishes of the genus *Sebastes* (Cuvier). *Mol. Phylog. Evol.* 44:790–811. [Article](#)
- Hyde, J. R., C. A. Kimbrell, J. E. Budrick, E. A. Lynn, and R. D. Vetter.
2008. Cryptic speciation in the vermilion rockfish (*Sebastes miniatus*) and the role of bathymetry in the speciation process. *Mol. Ecol.* 17:1122–1136. [Article](#)
- Jordan, D. S., and B. W. Evermann.
1898. The fishes of North and Middle America: a descriptive catalogue of the species of fish-like vertebrates found in the waters of North America, north of

- the Isthmus of Panama, part II. Bull. U.S. Natl. Mus. 47:1241–2183.
1900. The fishes of North and Middle America: a descriptive catalogue of the species of fish-like vertebrates found in the waters of North America, north of the Isthmus of Panama, part IV. Bull. U.S. Natl. Mus. 47:3137–3313 +pls.1–392.
- Jordan, D. S., B. W. Evermann, and H. W. Clark.
1930. Check list of the fishes and fishlike vertebrates of North and Middle America north of the northern boundary of Venezuela and Colombia. Rep. U.S. Comm. Fish. 1928, part II, 670 p.
- Jordan, D. S., and C. H. Gilbert.
1880a. Description of a new species of *Sebastichthys* (*Sebastichthys miniatus*) from Monterey Bay, California. Proc. U.S. Natl. Mus. 3:70–73.
1880b. Description of seven new species of sebastoid fishes, from the coast of California. Proc. U.S. Natl. Mus. 3:287–298.
1881. Description of *Sebastichthys mystinus*. Proc. U.S. Natl. Mus. 4:70–72.
1882. Synopsis of the fishes of North America. Bull. U.S. Natl. Mus. 16:1–1018.
- Jordan, D. S. and J. Z. Gilbert.
1919. Fossil fishes of the Miocene (Monterey) formations of Southern California. In Fossil fishes of Southern California, p. 13–60. Stanford Univ. Press, Stanford, CA.
1920. Fossil fishes of diatom beds of Lompoc, California, 45 p. + 39 pls. Stanford Univ. Press, Stanford, CA.
- Jordan, D. S. and P. L. Jouy.
1881. Check-list of duplicates of fishes from the Pacific coast of North America, distributed by the Smithsonian Institution in behalf of the United States National Museum, 1881. Proc. U.S. Natl. Mus. 4:1–18.
- Kramer, D. E., and V. O'Connell.
1995. Guide to northeast Pacific rockfishes genera *Sebastes* and *Sebastolobus*, 2nd rev. Alaska Sea Grant, Mar. Adv. Bull. 25, 78 p.
- Laidig, T. E., D. E. Pearson, and L. L. Sinclair.
2003. Age and growth of blue rockfish (*Sebastes mystinus*) from central and northern California. Fish. Bull. 101:800–808.
- Lenarz, W. H., and T. Wyllie Echeverria.
1991. Sexual dimorphism in *Sebastes*. In Rockfishes of the genus *Sebastes*: their reproduction and early life history (G. W. Boehlert and J. Yamada), p. 71–80. Springer Science+Business Media, Dordrecht, Netherlands.
- Love, M. S.
2011. Certainly more than you wanted to know about the fishes of the Pacific coast, a postmodern experience, 650 p. Really Big Press, Santa Barbara, CA.
- Love, M. S., M. Yoklavich, and L. Thorsteinson.
2002. The rockfishes of the northeast Pacific, 405 p. Univ. Calif. Press, Los Angeles, CA.
- Matsubara, K.
1934. Studies on the scorpaenoid fishes of Japan. I. Descriptions of one new genus and five new species. J. Imp. Fish Inst. Tokyo 30:199–210.
- Mecklenburg, C. W., T. A. Mecklenburg, and L. K. Thornsteinson.
2002. Fishes of Alaska, 1116 p. Am. Fish. Soc., Bethesda, MD.
- Miller, J. A., M. A. Banks, D. Gomez-Uchida, and A. L. Shanks.
2005. A comparison of population structure in black rockfish (*Sebastes melanops*) as determined with otolith microchemistry and microsatellite DNA. Can. J. Fish. Aquat. Sci. 62:2189–2198. [Article](#)
- Narum, S. R., V. P. Buonaccorsi, C. A. Kimbrell, and R. D. Vetter.
2004. Genetic divergence between gopher rockfish (*Sebastes carnatus*) and black and yellow rockfish (*Sebastes chrysomelas*). Copeia 2004:926–931. [Available at [website](#).]
- Orr, J. W., and J. E. Blackburn.
2004. The dusky rockfishes (Teleostei: Scorpaeniformes) of the North Pacific Ocean: resurrection of *Sebastes variabilis* (Pallas, 1814) and a redescription of *Sebastes ciliatus* (Tilesius, 1813). Fish. Bull. 102:328–348.
- Orr, J. W., M. A. Brown, and D. C. Baker.
2000. Guide to rockfishes (Scorpaenidae) of the genera *Sebastes*, *Sebastolobus*, and *Adelosebastes* of the North-east Pacific Ocean, 2nd ed. NOAA Tech. Memo. NMFS-SWFC-117, 47 p. [Available at [website](#).]
- Orr, J. W., and S. Hawkins.
2008. Species of the rougheye rockfish complex: Resurrection of *Sebastes melanostictus* (Matsubara, 1934) and a redescription of *Sebastes aleutianus* (Jordan and Evermann, 1898) (Teleostei: Scorpaeniformes). Fish. Bull. 106:111–134.
- Pallas, P. S.
1814. Zoographia Rosso-Asiatica, sistens omnium animalium in extenso Imperio Rossico et adjacentibus mari-bus observatorum recensionem, domicilia, mores et descriptiones anatomem atque icones plurimorum, vol. 3, 428 p. Acad. Sci. Imp., St. Petersburg, Russia.
- Phillips, J. B.
1957. A review of the rockfishes of California (Family Scorpaenidae). Calif. Dep. Fish Game, Fish. Bull. 104, 158 p.
- Pritchard, J. K., M. Stephens, and P. Donnelly.
2000. Inference of population structure using multilocus genotype data. Genetics 155:945–959.
- R Core Team.
2013. R: a language and environment for statistical computing. R Foundation for Statistical Computing, Vienna, Austria. [Available at [website](#), accessed May 2013.]
- Roques, S., D. Pallotta, J.-M. Sévigny, and L. Bernatchez.
1999. Isolation and characterization of polymorphic microsatellite markers in the North Atlantic redfish (Teleostei: Scorpaenidae, genus *Sebastes*). Mol. Ecol. 8:685–687. [Article](#)
- Sabaj Pérez, M. H. (ed.).
2013. Standard symbolic codes for institutional resource collections in herpetology and ichthyology: an online reference, version 4.0. [Available at [website](#), accessed June 2013].
- Schuelke, M.
2000. An economic method for the use of fluorescent labeling of PCR fragments. Nat. Biotechnol. 18: 233–234.
- Tilesius, W. G. von.
1813. Iconum et descriptionum piscium Camtschaticorum continuatio tertia tentamen monographiae generis *Agoni blochiani* sistens. Mem. Acad. Imp. Sci. St. Petersburg. 4:406–478.
- VenTresca, D. A., R. H. Parrish, J. L. Houk, M. L. Gingras, S. D. Short, and N. L. Crane.
1995. El Niño effects on the somatic and reproductive condition of blue rockfish, *Sebastes mystinus*. CalCOFI Rep. 36: p. 167–174.

- Warton, D. I., R. A. Duursma, D. S. Falster, and S. Taskinen.
2012. smatr 3—an R package for estimation and inference about allometric lines. *Methods Ecol. Evol.* 3:257–259. [Article](#)
- Westerman, M. E., V. P. Buonaccorsi, J. A. Stannard, L. Galver, C. Taylor, E. A. Lynn, C. A. Kimbrell, and R. D. Vetter.
2005. Cloning and characterization of novel microsatellite DNA markers for the grass rockfish, *Sebastes rastrelliger*, and cross-species amplification in 10 related *Sebastes* spp. *Mol. Ecol. Notes* 5:74–76. [Article](#)
- Whiteaves, J. F.
1887. On some marine Invertebrata dredged or otherwise collected by Dr. G.M. Dawson, in 1885, on the coast of British Columbia; with a supplementary list of a few land and fresh water shells, fishes, birds, etc., from the same region, 137 p. Dawson Brothers Publishers, Montreal, Canada.
- Wickham, H.
2009. ggplot2: elegant graphics for data analysis, 213 p. Springer, New York.
- Wyllie Echeverria, T.
1986. Sexual dimorphism in four species of the rockfish genus *Sebastes* (Scorpaenidae). *Environ. Biol. Fish.* 15:181–190. [Article](#)
1987. Thirty-four species of California rockfishes: maturity and seasonality of reproduction. *Fish. Bull.* 85:229–250.
- Yoshida, K., M. Nakagawa, and S. Wada.
2005. Multiplex PCR system applied for analysing microsatellite loci of Schlegel's black rockfish, *Sebastes schlegeli*. *Mol. Ecol. Notes* 5:416–418. [Article](#)